RESEARCH ARTICLE

Key Points:
- Early Jurassic rifting between Africa and Antarctica took place in a WNW-ESE direction
- Eastern part of the Mozambique Coastal Plain is underlain by oceanic crust

Correspondence to:
L. C. Nguyen,
lcnguyen4@uh.edu

Reconstruction of the East Africa and Antarctica continental margins

**Luan C. Nguyen[1], Stuart A. Hall[1], Dale E. Bird[1,2], and Philip J. Ball[3]**

[1]Department of Earth and Atmospheric Sciences, University of Houston, Houston, Texas, USA, [2]Bird Geophysical, Houston, Texas, USA, [3]ConocoPhillips Company, Houston, Texas, USA

Abstract The Early Jurassic separation of Antarctica from Africa plays an important role in our understanding of the dispersal of Gondwana and Pangea. Previous reconstruction models contain overlaps and gaps in the restored margins that reflect difficulties in accurately delineating the continent-ocean-boundary (COB) and determining the amount and distribution of extended continental crust. This study focuses on the evolution of the African margin adjacent to the Mozambique Basin and the conjugate Antarctic margin near the Riiser-Larsen Sea. Satellite-derived gravity data have been used to trace the orientations and landward limits of fracture zones. A 3-D gravity inversion has produced a crustal thickness model that reliably quantifies the extent and amount of stretched crust. Crustal thicknesses together with fracture zone terminations reveal COBs that are significantly closer to the African and Antarctic coasts than previously recognized. Correlation of fracture zone azimuths and identified COBs suggests Antarctica began drifting away from Africa at approximately 171 Ma in a roughly SSE direction. An areal-balancing method has been used to restore the crust to a uniform prerift thickness so as to perform a nonrigid reconstruction for both nonvolcanic and volcanic margins. Both margins reveal a trend of increasing extension from east to west. Our results suggest Africa underwent extension of 60–120 km, while Antarctic crust was stretched by 105–180 km. Various models tested to determine the direction of extension during rifting suggest that Antarctica moved away from Africa in a WNW-ESE direction during the period between 184 and 171 Ma prior to the onset of seafloor spreading.

1. Introduction

In all rigid-plate tectonic models of Gondwana the relationship between Antarctica and Africa plays a fundamental role in the positioning of the main plates of East Gondwana (Figure 1) [*Seton et al.*, 2012; *Gaina et al.*, 2015]. The conjugate margins of Africa and Antarctica are best observed in the Mozambique Basin, Africa, and the Riiser-Larsen Sea, Antarctica (Figure 2). Unfortunately, the early breakup history is difficult to decipher because magmatic/volcanic processes overprint and mask the rifting fabric and may thicken the early oceanic crust domains, making it difficult to interpret magnetic seafloor spreading anomalies. The syn-tectonic breakup of Gondwana is associated with a long history of episodic volcanism that left behind several large igneous Provinces. Due to the temporal association between these volcanic events and timing of continental breakup, it has been postulated that they are the driving force behind continental rifting and subsequent drifting of Gondwana's subcontinents [*Encarnación et al.*, 1996; *Duncan et al.*, 1997].

Onshore Africa geology adjacent to the Mozambique Basin includes the Mozambique Province and the Mozambique Coastal Plain. The Mozambique Province is described as a cratonic terrain consisting of ~1000 Ma igneous and metasedimentary and volcanic basement [*Groenewald et al.*, 1991]. The Mozambique Coastal Plain (MCP) is bounded to the west and northwest by the Lebombo and the Mateke-Sabi monoclines, respectively. These are volcanic remnants of the Karoo eruptions. Landward of these monoclines are the Zimbabwe and Kaapvaal provinces which have Archaean to mid-Proterozoic basement [*Groenewald et al.*, 1991]. The MCP itself is covered by sedimentary layers that postdate the Karoo volcanism which took place during the period of 184–173 Ma [*Duncan et al.*, 1997; *Cox*, 1992]. The underlying crust of the MCP has been interpreted as thickened oceanic crust [*Watts*, 2001; *Leinweber and Jokat*, 2011; *Eagles and König*, 2008] or thinned continental crust [*König and Jokat*, 2010; *Cox*, 1992]. Exploration wells drilled at this area terminated against basalt layers that are estimated from sedimentation rate to be in the age range of 175–140 Ma [*Flores*, 1973; *Kamen-Kaye*, 1983]. The onshore geology of Dronning Maud Land adjacent to the Riiser-Larsen Sea, Antarctica consists of three different basement domains: (1) the 3 Ga Archean Grunehogna craton, which has some affinity to the Kaapvaal Province in southeast Africa, (2) the Sor Rodane, and (3) the Muhlig-Hofmannfjella terrain. The former has an approximate age of 1000–1200 Ma,
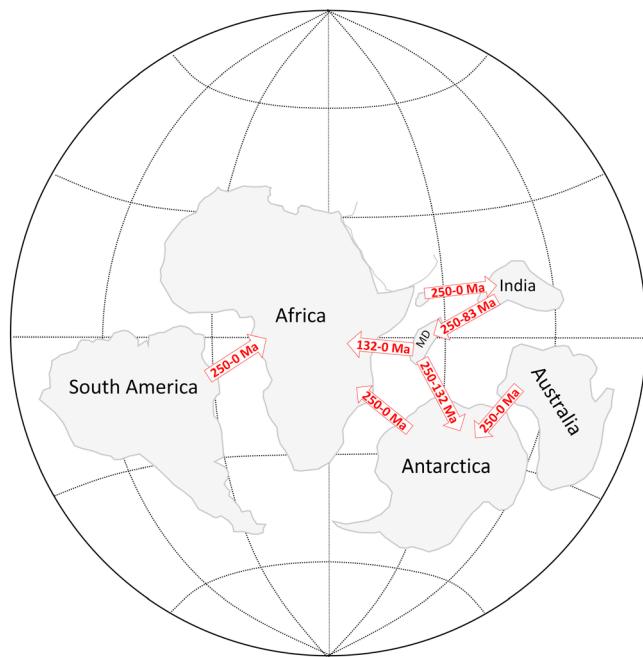
Figure 1. Illustration showing the reconstruction circuit among continents of Gondwana from *Seton et al.* [2012]. Red arrows point to the anchor plates with red numbers indicate the time interval during which a particular plate is reconstructed with respect to its anchor plate. Numbers in parentheses are plate identification numbers assigned in GPlates. Note that every continent of Gondwana is tied to either Africa or Antarctica which in turn are linked together in the reconstruction model.

the latter is closer to the East African orogeny 500–650 Ma [*Grantham et al.*, 2008; *Marschall et al.*, 2010] (Figure 3).

Multiple studies over the last 50 years have investigated the tectonic evolution of Africa and Antarctica [e.g., *Bergh*, 1977; *Norton and Sclater*, 1979; *Rabinowitz et al.*, 1983; *Martin and Hartnady*, 1986; *Roeser et al.*, 1996; *Jokat et al.*, 2003; *Cox*, 1992; *Reeves and de Wit*, 2000; *Eagles and König*, 2008; *Leinweber and Jokat*, 2012; *Seton et al.*, 2012; *Gaina et al.*, 2013; *Gaina et al.*, 2015]. There is a general consensus that the timing of breakup is somewhere between 170 and 160 Ma. Despite these many studies, numerous issues remain regarding details of the plate kinematic evolution during the early breakup and rift history of Africa-Antarctica. Within the Africa-Antarctica corridor, offshore, symmetrical well-defined magnetic anomalies older than M25 remain elusive [*Leinweber and Jokat*, 2012]. Thus, a confident pre-breakup fit of the two continents remains poorly constrained. In addition, enigmatic crustal blocks, such as the Beira High and the Mozambique Ridge along
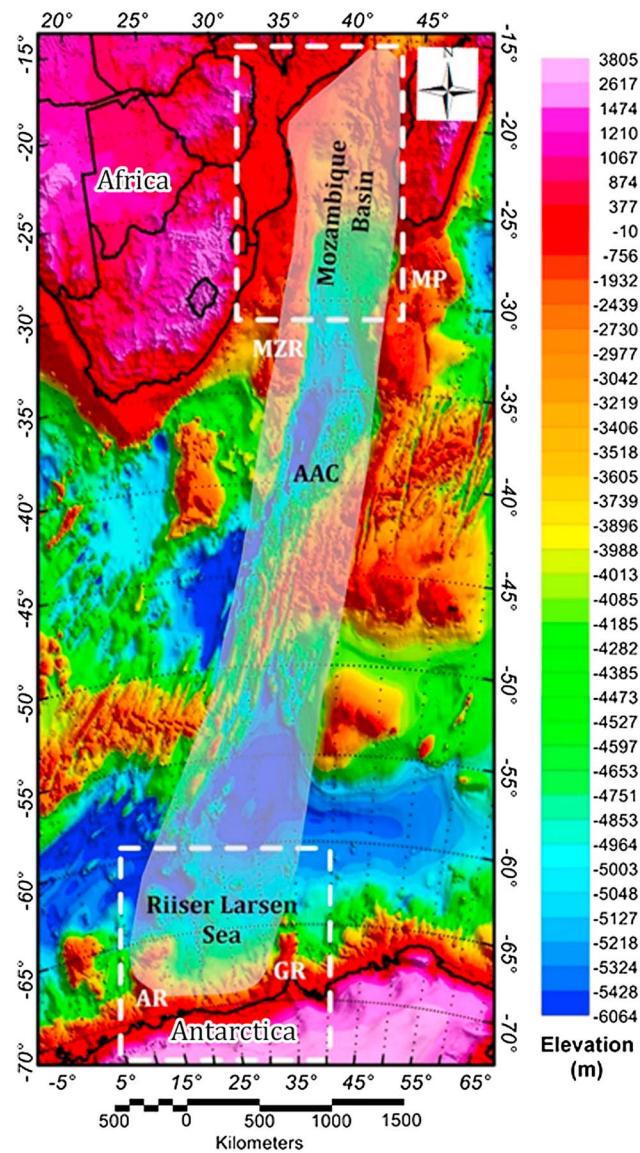
the African margin and the Astrid Rise and Gunnerus Ridge from the Antarctic conjugate margin, confound the early breakup and prerift configurations (Figure 3).

The origin of the Mozambique Ridge (MZR) is still a matter of debate. Several studies have presented conflicting support for either a continental or oceanic structure [*Leinweber and Jokat*, 2011; *König and Jokat*, 2010; *Tucholke et al.*, 1981; *Simpson et al.*, 1979; *Hales and Nation*, 1972; *Chetty and Green*, 1977]. Dredged samples along the edge of the ridge returned Precambrian rocks even though there is no radiometric dating available for these samples [*Mougenot et al.*, 1991; *Hartnady et al.*, 1992; *Ben-Avraham et al.*, 1995]. *König and Jokat* [2010] proposed that it consists of an oceanic core surrounded by continental fragments and proposed that the MZR was produced as excess volcanism during a series of ridge jumps. The Beira High is another significant structure, whose origin is also debated. Detailed gravity modeling from *Watts* [2001] points to a thickened oceanic crust flooring the Beira High, whereas seismic reflection study of *Mahanjane* [2012] suggests this is a continental structure. The composition of the Beira High is crucial in restoring the conjugate margins of Africa and Antarctica since it controls the determination of the location of continent-ocean boundary in the western Mozambique Basin.

On the conjugate margin of Antarctica within the Riiser-Larsen Sea, pronounced geologic features include the Astrid and Gunnerus Ridges (Figure 3). From seismic and potential field studies, the Astrid Ridge has been interpreted as an oceanic structure which is separated into northern and southern parts by the Astrid Fracture Zone [*Bergh*, 1987; *Roeser et al.*, 1996; *Hinz et al.*, 2004; *Jokat et al.*, 2004; *Leinweber and Jokat*, 2012]. *Leinweber and Jokat* [2012] revealed that the two parts of the Astrid Ridge expressed significantly different magnetic signatures and thus might have formed at different times or by different mechanisms. The Gunnerus Ridge marks the eastern boundary of the Riiser-Larsen Sea and has been the subject of seismic and potential field studies [*Saki et al.*, 1987; *Hinz et al.*, 2004; *Leitchenkov et al.*, 2008], as well as dredged samples [*Saki et al.*, 1987]. Continental crust is ascribed to the Gunnerus Ridge based on its top basement seismic velocity of 5.1–6.1 km/s and autochthonous metamorphic debris sample at the ridge [*Leitchenkov et al.*, 2008; *Saki et al.*, 1987]. Different ages of volcanic extrusion are identified along the Antarctic margin. The inner seaward
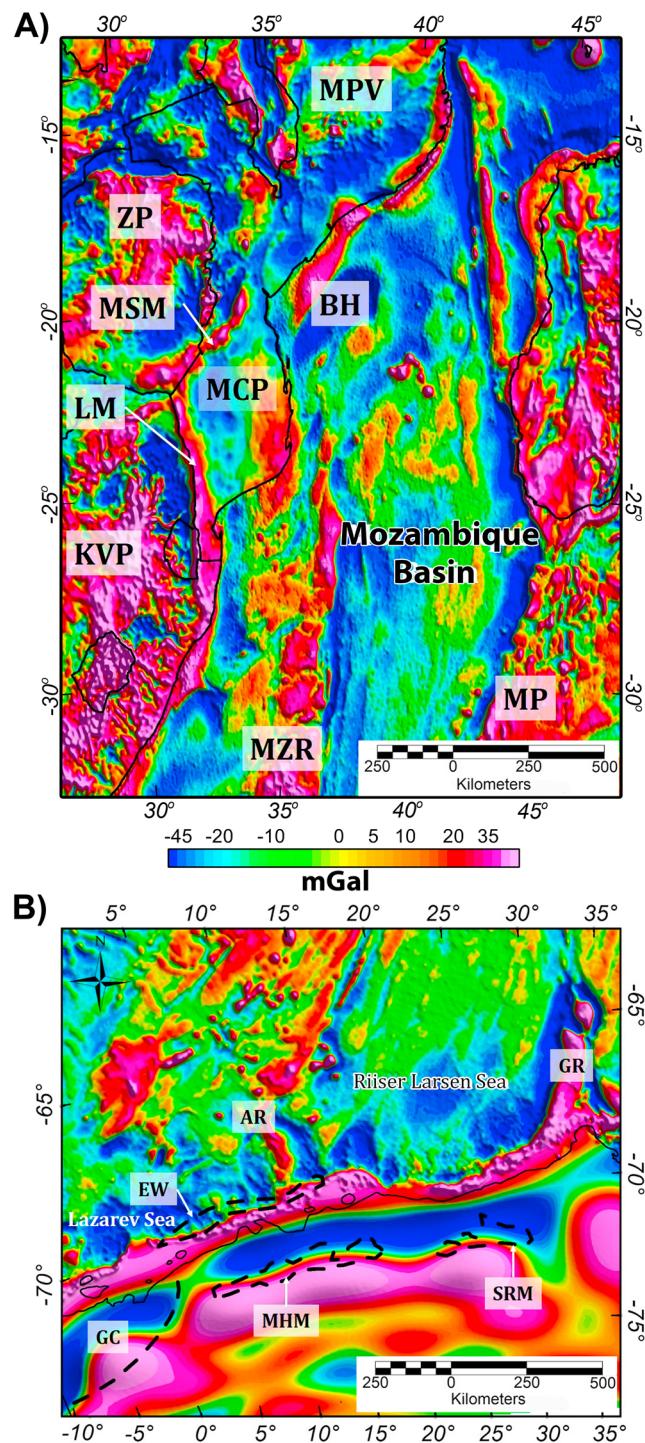
Figure 2. Location map, overlay of topography (National Geophysical Data Center and U.S. Geological Survey), showing the Africa-Antarctica corridor extending from the Mozambique Basin to the Riiser-Larsen Sea. This zone contains oceanic crust formed during the drifting of Antarctica from Africa. Dashed white boxes indicate locations of the Mozambique Basin in the north and the Riiser-Larsen Sea in the south with their adjacent onshore areas. MZR: Mozambique Ridge, MP: Madagascar Plateau, AR: Astrid Ridge, and GR: Gunnerus Ridge. Map projection: Albert conic, equal area.

dipping reflectors (SDRs) are thought to be contemporaneous with the Karoo volcanism observed onshore Africa and are considered as conjugate features of the Lebombo and Mateke-Sabi monoclines in different reconstruction models [*Cox*, 1992; *Martin and Hartnady*, 1986]. However, its outer formations are considered to be younger (150–138 Ma) and formed sometime after the initial breakup event [*König and Jokat*, 2010].

Though tremendous efforts have been devoted to decoding the breakup history of Gondwana, there are still gaps in our knowledge regarding the timing and geometry of the breakup. The previously proposed final fit of the conjugate margins often contains overlaps or gaps that reflect different interpretations of the COBs and the difficulty in determining the distribution of extended continental crust [*Eagles and König*, 2008; *Reeves and De Wit*, 2000; *Marks and Tikku*, 2001; *Seton et al.*, 2012] (Figure 4). *Eagles and König* [2008] reconstructed the African-Antarctic margin to 183 Ma by fitting gravity anomalies that they interpreted as the landward limit of the conjugate margins. In this model, the Mozambique Ridge was considered a continental fragment and restored to onshore Africa, while the Mozambique Coastal Plain was considered to be oceanic. Similarly, *Marks and Tikku* [2001] treated the Mozambique Coastal Plain as oceanic; however, they only proposed a prebreakup fit at 165 Ma based on the seafloor magnetic anomalies. The full-fit model at 200 Ma of *Reeves and De Wit* [2000] was achieved by correlating crustal structures on the African and Antarctic sides, this model led to a large overlap of the interpreted COBs, which they argued represented extended crust within

the rifted zones between continental fragments. *Seton et al.* [2012] restored the margin to 160 Ma by using the gridded seafloor magnetic isochrons of *Müller et al.* [2008]. In this model the 160 Ma reconstruction produces large overlaps of the interpreted COB between the African-Antarctic margin. Up to this point, no quantitative study to account for the extension during rifting has been conducted. This study reexamines the fracture zone interpretations utilizing the latest version of the Sandwell and Smith gravity anomalies (V23.1 in *Sandwell et al.* [2014]) and magnetic anomalies [*Maus et al.*, 2007] to determine the COB in the East African margins along the Mozambique Basin and the Riiser-Larsen Sea in the conjugate margin of Antarctica. We examine prerift fits of Antarctica and Africa by testing nonrigid-plate models that account for the observed crustal thickness. We apply volumetric based crustal corrections to determine a prerift fit, considering both nonvolcanic and volcanic

Figure 3. Free-air gravity anomaly map [*Sandwell et al.*, 2014] of (a) the Mozambique Basin and its adjacent structures. BH: Beira High, LM: Lebombo Monocline, KVP: Kaapvaal Province, MCP: Mozambique Coastal Plain, MP: Madagascar Plateau, MPV: Mozambique Province, MSM: Mateke-Sabi Monocline, MZR: Mozambique Ridge, and ZP: Zimbabwe Province (b) The Riiser-Larsen Sea area. AR: Astrid Ridge, EW: Explora Wedge SDR, GC: Grunehogna Craton, GR: Gunnerus Ridge, MHM: Muhlig-Hofmannfjella Mountain, and SRM: Sor Rodane Mountain. Map projection: Albert conic, equal area.

thickening through extrusive and intrusive magmatism of the margins. Crustal thickness is determined using combined seismic refraction and 3-D gravity inversion results and depth to basement maps for both conjugate margins. Consequently, the amount of continental stretching and errors relating to this is quantified using different prerift thicknesses. The final result is to achieve a prerift restoration of the African and Antarctic margins prior to rifting.

2. Data and Methods

2.1. Three-Dimensional Gravity Inversion

The gravity inversion approach of this study is similar to that used to estimate crustal thickness in other parts of the world [*Williams et al.*, 2011; *Hosseinpour et al.*, 2013; *Bai et al.*, 2015]. A five layer 3-D model was constructed from four horizons: topography, seawater surface, top of crystalline basement, and the base of the crust (Moho). Onshore global GTOPO30 (30 arc sec grid) and the offshore portion of the global TerrainBase (5 arc min grid) were merged. These data sets are accessible through the United States Geological Survey website. It is important not to use ETOPO1 or ETOPO2 topographic grids because they were created, in part, from gravity data [*Smith and Sandwell*, 1997].

Two global sediment thickness grids can be downloaded from the National Geophysical Data Center (offshore only, 5 arc min grid) and the University of California, San Diego (onshore and offshore, 1 arc degree grid). These grids were merged by replacing the offshore part of the 1 arc degree grid with the 5 arc min grid to retain the best resolution for both onshore and offshore. Sedimentary thickness was used as the basis to calculate depth to top of crystalline basement which was also further calibrated using publicly available seismic reflection and refraction data, and isopach map in the Mozambique Basin [*Leinweber et al.*, 2013; *Mahanjane*, 2012; *Buyl and Flores*, 1986], as well as local isopach map in the Riiser-Larsen Sea [*Leitchenkov et al.*, 2008].
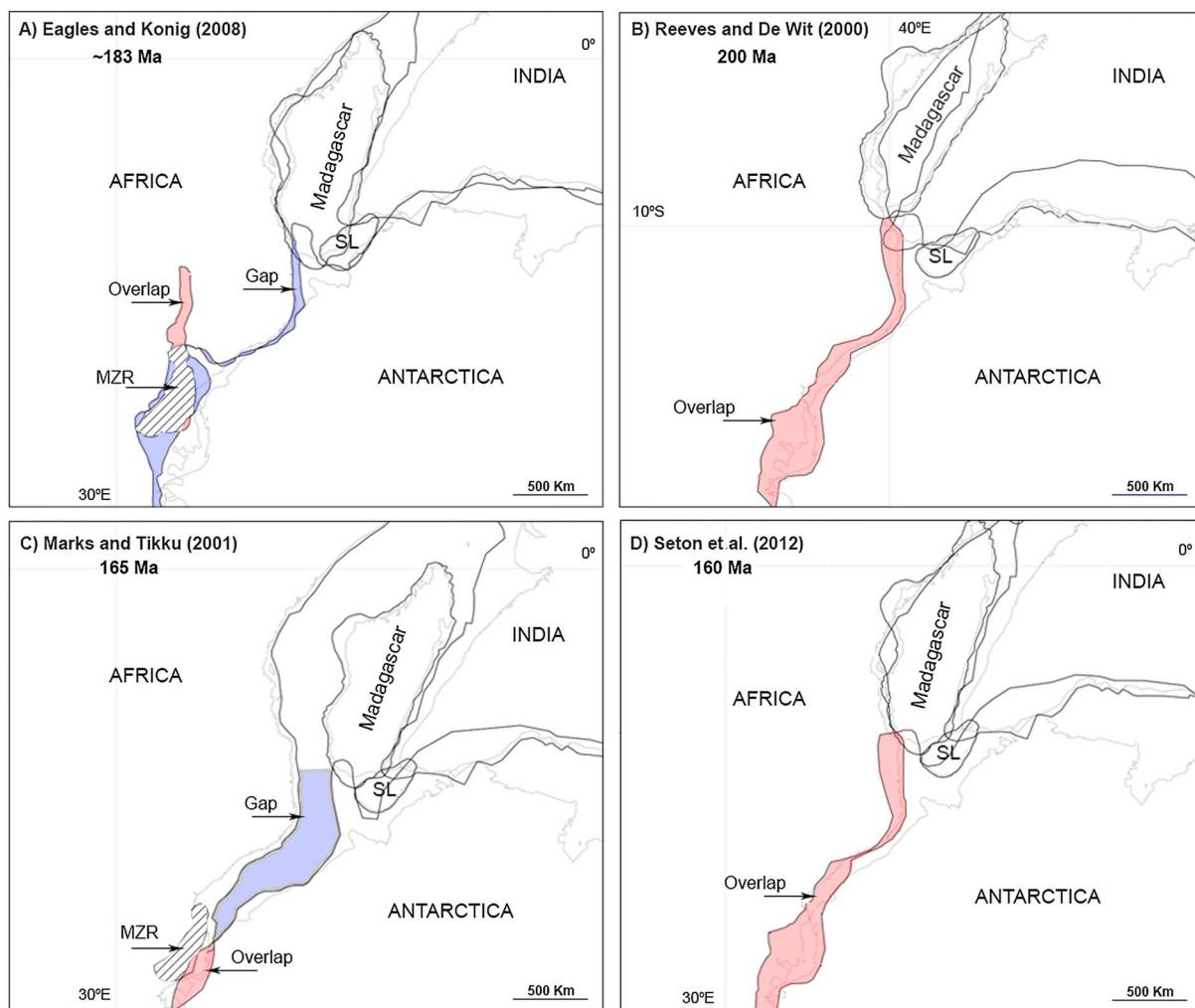
Figure 4. Full-fit reconstruction models for East Gondwana with highlighted overlaps and gaps between Africa and Antarctica. (a) *Eagles and König* [2008] restored the margins using "gravity isochrons." (b) Reconstruction of *Reeves and de Wit* [2000] was based on correlation of geological units from Africa, Antarctica, and Madagascar. No quantification for the overlap area was provided from these studies. (c) The model of *Marks and Tikku* [2001] proposed a prebreakup fit at 165 Ma that resulted in a large gap between Africa and Antarctica as well as Africa and Madagascar. (d) Reconstruction model at 160 Ma from *Seton et al.* [2012] using gridded seafloor magnetic isochrons. MZR denotes Mozambique Ridge. Solid dark lines are present-day COBs. SL: Sri Lanka.

The Moho horizon was created using an Airy isostatic calculation [*Blakely*, 1995]. The calculation was modified by using heat flow versus oceanic crust age as a proxy to scale the application of the isostatic correction [*Sclater et al.*, 1980; *Müller et al.*, 2008]. This is because seafloor spreading centers are often topographically elevated, and a 100% application of the correction would produce a crustal root beneath the spreading center.

Air, water, and crystalline crust layers were assigned constant densities: 0.0, 1.03, and 2.85 g/cc, respectively. To account for the effect of compaction, the sedimentary layer was assigned a variable density based on thickness and water depth following *Sykes* [1996]. For Antarctica, a layer of ice sheet with density of 0.93 g/cc is also incorporated into the model. Ice thickness (Bedmap2) is publicly available from the British Antarctic Survey website. The upper mantle density was scaled from 3.1 beneath the spreading center to 3.35 away from the spreading center, also using heat flow versus oceanic crust age [*Sclater et al.*, 1980].

A structural gravity inversion on the Moho horizon was then calculated using an algorithm described by *Parker* [1973]. A crustal thickness model was derived from the inverted Moho depth and top of basement horizons.

2.2. Locations of the Continent-Ocean Boundaries (COBs)

COBs in the conjugate margins of Africa and Antarctica are important parameters for both rigid and nonrigid reconstructions. Positive magnetic anomalies have been proposed as indicators of the continent-ocean

Table 1. Cross Sectional Areas of Seaward Dipping Reflectors (SDR) and/or Basalt Flows and Their Corresponding Areas of Magmatic Underplating in Different Volcanic Margins Around the World

Margin	SDR (km^2)	Underplating (km^2)	SDR/Underplating (%)	Source
Namibia	580	953	60	*Bauer et al.* [2000]
Namibia	356	690	51	*Bauer et al.* [2000]
Greenland	544	1840	29.5	*Voss and Jokat* [2007]
Greenland	500	1880	27	*Schnabel et al.* [2008]
Argentina	102	395	26	*Schnabel et al.* [2008]
Norway	232	517	45	*Mjelde et al.* [2005]
		Average	40	

boundaries in other rifted margins such as the eastern U.S. [*Hutchinson et al.*, 1983; *Austin et al.*, 1990], southern Brazil [*Rabinowitz and Labrecque*, 1977], and northwestern Australia [*Veevers et al.*, 1985]. In addition, because the difference between the thickness of oceanic and continental or transitional crusts is quite considerable, locating an abrupt change in crustal thickness along a continental margin is also a good indicator for the COB. Lastly, fracture zones are oceanic structures directly associated with transform boundaries on a spreading center, thus their presence is strong evidence for oceanic crust. Utilizing the preceding observations on the nature of COBs, this study interprets magnetic anomaly, changes in crustal thickness, and fracture zone traces to determine locations of the COBs in the study areas.

Crucial to this study is the new version (V23.1) of satellite-derived free-air gravity anomaly data published in *Sandwell et al.* [2014]. With its improved resolution, fracture zone traces become more visually detectable. A tilt-derivative filter [*Verduzco et al.*, 2004] was applied to this data set to highlight the fracture zone trends.

2.3. Rigid Reconstruction

The reconstruction of Antarctica back to its position prior to the initiation of seafloor spreading is performed by visual fitting of (1) magnetic anomaly picks from M0r (124.8 Ma) to M22n1n (149.5 Ma) published in *Leinweber and Jokat* [2012], (2) our interpreted fracture zones, and (3) our interpreted COBs in the conjugate margins. Plate rotations were conducted using GPlates 1.5 software application.

2.4. Nonrigid Reconstruction

Multiple 2-D cross sections across the conjugate continental margins are extracted from the 3-D model. The amount of continental extension is estimated by calculating the area of vertical slices that extend from prerift boundaries to the COBs. The prerift boundary is assumed to be where the crust has a thickness of 42 km from the 3-D gravity inversion. Different values for unstretched crustal thickness were examined but 42 km yielded the lowest misfit between the restored prerift boundaries over the conjugate margins (see section 3.4). The area of crust between the boundaries is calculated. The inner boundary is assumed to be where present day we observe a crustal thickness of 42 km. The outer boundary is delineated by the interpreted COB. This area is maintained as each cross section is collapsed by progressively moving the continent-ocean boundary landward until the crustal thickness is everywhere uniform and equal to the original, undeformed thickness of 42 km. Subsequently, the conjugate prerift boundaries were restored by visually matching them together to determine the full-fit plate geometry. Such method of areal balancing has been used by *Sutra et al.* [2013] and *Williams et al.* [2011] to restore the conjugate margins between Iberia and Newfoundland, and Australia and Antarctica, respectively. Because magmatic underplating probably occurred in the region [*Leinweber et al.*, 2013], several magmatic margins have been studied to estimate the ratio between the thickness of seaward dipping reflectors (SDRs) and that of magmatic underplating (Table 1). The estimated amount of underplating is removed from total crustal area prior to the collapse of cross sections to prerift thickness. For example, if material was added to the base of the crust after or during continental extension, then the restored COB would be farther inboard than it would be without the added material.

3. Results
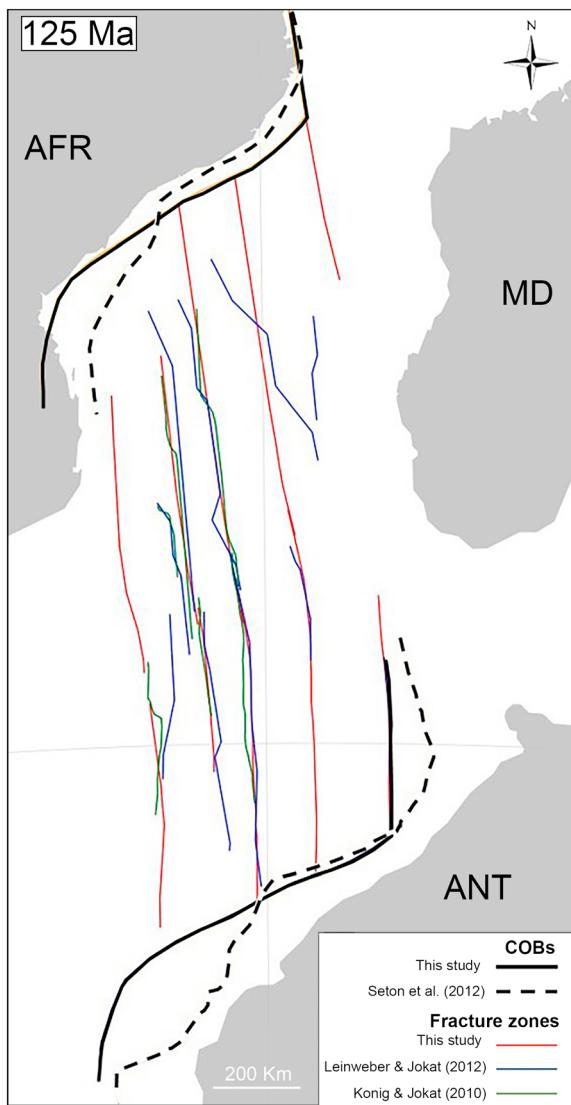
3.1. Fracture Zone Tracing

Figure 4 shows the tilt derivative [*Miller and Singh*, 1994; *Verduzco et al.*, 2004] of residual gravity anomaly maps which were generated by subtracting the 30 km upward continued Bouguer gravity anomaly from
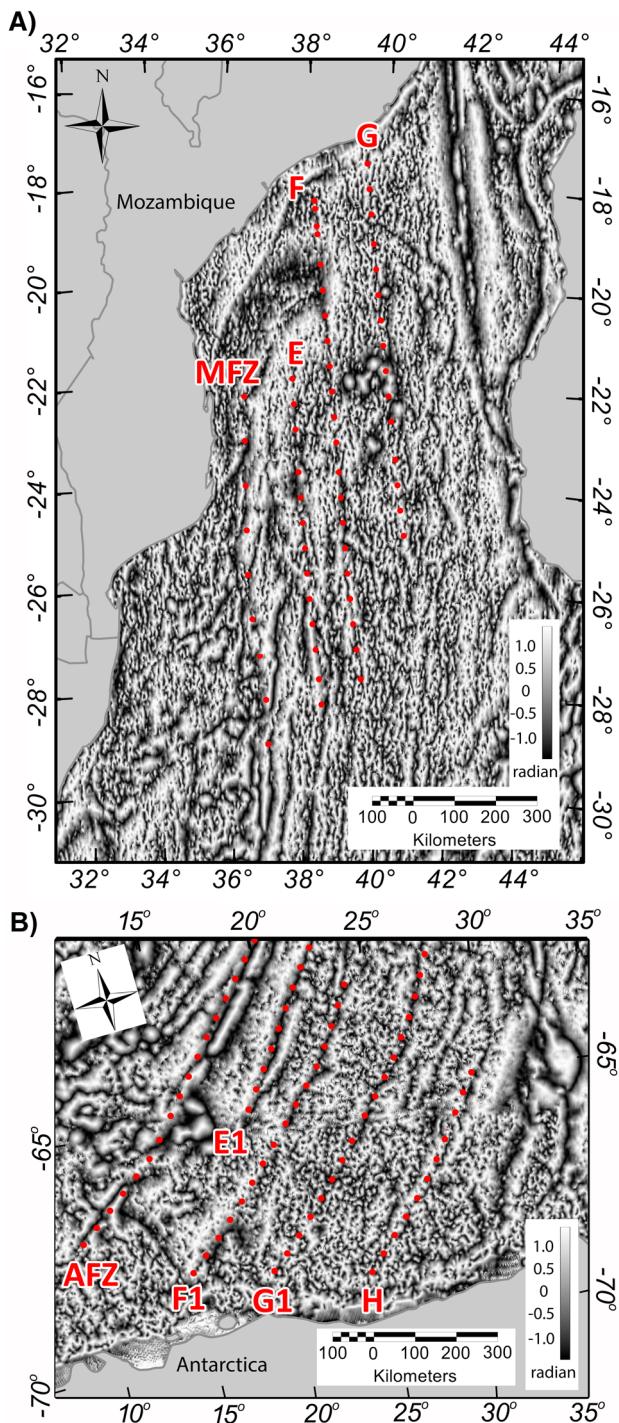
Figure 5. Tilt-derivative filter applied to 30 km residual gravity anomaly data over (a) the Mozambique Basin. Note the roughly N-S linear trends that are subparallel to the Davie Fracture Zone (dashed outline). The sparsely dotted lines are interpreted fracture zones referred to as Mozambique Fracture Zone (MFZ), fracture zones E, F, and G. (b) The Riiser-Larsen Sea. NE-SW linear trends are visible at 65°S and areas farther north but faint toward the coastline. The dotted lines are interpreted fracture zones. Beside the most clearly defined Astrid Fracture Zones (AFZ), from left to right, are fracture zone E1, F1, G1, and H. Map projection: Albert conic, equal area.

the derived Bouguer gravity anomaly. This filtering process helps delineate anomalies caused by density contrasts from within the upper crust. Distinctly recognized in these maps are the fracture zones extending from the mid-ocean ridge to the continental margins of Africa and Antarctica. Of the four fracture zones identified over the Mozambique Basin (Figure 5a), three have been partly recognized as the Mozambique Fracture Zone (MFZ) and fracture zones E and F through previous gravity and magnetic anomaly interpretation [*Segoufin*, 1978; *Simpson et al.*, 1979; *König and Jokat*, 2010; *Leinweber and Jokat*, 2012]. A new fracture zone identified from this study is fracture zone G which is about 140 km east of fracture zone F. All four identified fracture zones have subparallel N-S trends. The northern end of fracture zones F and G can be confidently traced northward to about 16°N, 70 km off the coast of Mozambique. Fracture zone E may extend as far north as the southern edge of the Beira High even though the gravity signature becomes noisy as it approaches the structure. The MFZ is traced from 22°N at about 80 km east of southern Mozambique and extends roughly N-S to 28°N where it slightly bends to the west and continues along the eastern edge of the Mozambique Ridge. To the south, the fracture zones terminate at 25–28°S where they join with another set of fracture zones that have a different orientation connecting the Mozambique Basin and the mid-ocean ridge in a NE-SW direction.

Similarly, the Riiser-Larsen Sea is separated into a number of sea floor spreading corridors by five recognized fracture zones (Figure 5b). In the western end is the Astrid Fracture Zone [*König and Jokat*, 2010; *Leinweber and Jokat*, 2012] that trends NE-SW from the mid-ocean ridge to the Riiser-Larsen Sea and bifurcates the Astrid Ridge into northern and southern parts. The other four fracture zones have also been partially distinguished by previous gravity and magnetic studies [*Bergh*, 1977; *König and Jokat*, 2010; *Leinweber and Jokat*, 2012]. Nevertheless, the new gravity data enable this study to extend these fracture zones much farther south toward the continental margin of Antarctica. In this

Figure 6. Comparison of fracture zones and COBs with previous studies. Fracture zones from this study are traced farther toward the continental margins of Africa and Antarctica and, therefore, help constrain plate motion during early drifting.

study, these fracture zones are termed E1, F1, G1, and H1 from west to east. They are subparallel in a more NE-SW direction and can be traced as far south as 67°S, approximately 75 km offshore Antarctica. Figure 6 compares the fracture zones identified in this study to those previously proposed in the Mozambique Basin and the Riiser-Larsen Sea.

3.2. Three-Dimensional Gravity Inversion

The inversion algorithm of *Parker* [1973] incorporated in this study was shown be sensitive to the input parameters including initial values for Moho depth (*Mdepth*) and density contrast across the Moho ($\Delta\rho$) [*Hosseinpour et al.*, 2013]. Different combinations of Mdepth, including a calculated isostatic Moho surface, and $\Delta\rho$ were tested with gravity inversion. The gravity-inverted Moho depths were then compared with those estimated from seismic methods throughout the study area [*Leinweber and Jokat*, 2012; *Parsiegla et al.*, 2009; *Leitchenkov et al.*, 2008; *Hinz et al.*, 2004; *Gohl and Uenzelmann-Neben*, 2001; *Hirsch et al.*, 2009; *Barret*, 1977; *Chave*, 1979; *Qui et al.*, 1996; *Nguuri et al.*, 2001; *Webb et al.*, 2004; *Nain et al.*, 2006; *Zhao et al.*, 1999; *Li et al.*, 2003; *Gore et al.*, 2009; *Fourno*, 1987; *Bertill and Regnoult*, 1998; *Sinha et al.*, 1981; *Kydryavtzev et al.*, 1991; *Ikami et al.*, 1983, 1984; *Kurinin and Grikurov*, 1982; *Bauer et al.*, 2000; *Green and Hales*, 1966; *Hales and Nation*, 1972; *Hayes et al.*, 1991; *Goslin et al.*, 1981; *Tucholke et al.*, 1981; *Steinhar and Meyer*, 1961; *Huebscher et al.*, 1996; *Bentley*, 1991; *Baier et al.*, 1983; *Green and Durrheim*, 1990; *Stuart and Zengeni*, 1987; *Durrheim et al.*, 1992; *Recq et al.*, 1998; *Hales and Sacks*, 1959; *Bloch et al.*, 1969; *Ludwig et al.*, 1968; *Kogan*, 1972]. Results from the sensitivity test are shown in Table 2. Initial Mdepth at 25 km with $\Delta\rho$ of 500 km/m^3 yields the lowest root-mean-square (RMS) and average misfits (Figure 7). Moho depths inverted from this combination of Mdepth and $\Delta\rho$ were used to compute the final crustal thickness of this study.

The error grid which is the difference between the observed data and the calculated gravity anomaly is shown in Figure 8. The mean misfit is about 1.5 mGal with a standard deviation of about 15.2 mGal. The maximum and minimum misfits are 275.2 mGal and −132.0 mGal, respectively. High misfits are observed in areas close to the mid-ocean ridge, whereas the continents and their margins have maximum difference of about 40 mGal. The anomalously high misfit at the mid-ocean ridge could be due to underestimated mantle density (3.0 g/cc). Nevertheless, these misfits can be tolerated as the crustal thickness at the mid-ocean ridge is not involved in the rigid and nonrigid reconstructions. More importantly, over the Mozambique Basin and Mozambique continental margin, the average difference is less than 10 mGal with the maximum misfit of about 40 mGal close to the shelf break along 15–17°S. Here the lower than observed gravity anomaly calculated from the model might suggest higher density should be used for the sediment package. Presence of magmatic material that is not incorporated in the model might also produce such a misfit. This misfit could

Table 2. Sensitivity Test of Gravity Inversion With Different Combinations of $\Delta\rho$ and Mdepth[a]

$\Delta\rho$ (kg/m^3)	400					450					500				
Mdepth (km)	22	25	28	31	Isostatic	22	25	28	31	Isostatic	22	25	28	31	Isostatic
RMS error (km)	6.6	7.4	9.2	11.5	9.3	6.3	6.6	8.1	10.3	8.3	6.4	6.2	7.4	9.4	7.7
Average error (km)	5.1	5.8	7.6	9.9	7.7	4.8	5.1	6.7	8.9	6.9	4.8	4.9	6.2	8.2	6.4

[a]The smallest RMS error between depth of gravity-inverted Moho and seismic Moho results from $\Delta\rho$ of 500 kg/m^3 and Mdepth of 25 km. "Isostatic" denotes laterally variable Moho grid calculated using the principle of isostasy.

affect depth of the inverted Moho and thus the crustal thickness. Favorably, in this area where the observed and calculated have a large difference, there are seismic refraction profiles that can be used to test the inversion results and account for inaccurate crustal thickness (Figure 9). On the other hand, the calculated gravity anomaly from the model's response is in very good agreement with the observed data over the Riiser-Larsen Sea and Antarctic margin where misfit values are in range of only a few mGal. To produce a more geologically plausible Moho, a low pass filter was applied to the inverted Moho to reduce or eliminate spiky and abrupt changes in Moho depth that have wavelengths less than 50 km.

Crustal thickness calculated by subtracting the inverted Moho from the basement grid is shown in Figure 9. Onshore African and Antarctic continents, the average crustal thicknesses are about 40 km and 44 km, respectively. In the central Mozambique Basin and Riiser-Larsen Sea, the crust is about 7 to 11 km thick. In the deep ocean basins beyond the continental margins, crustal thickness ranges from 4.5 to 7 km. Submarine plateaus (Maud Rise, Madagascar Plateau, Astrid Ridge, etc.,) are 20 km thick on average. In general, the resulting values are consistent with findings from seismic studies in Africa and Antarctica as well as the global average for crustal thickness of various structures [*Mooney et al.*, 1998; *Baranov and Morelli*, 2013].

Quality control of the inversion results was carried out using two seismic refraction profiles from *Leinweber et al.* [2013] in the Mozambique margin (Figures 10a and 10b) and another pair of refraction-constrained gravity models from *Leitchenkov et al.* [2008] (Figures 10c and 10d) over the Antarctic margin. Over the Mozambique Basin, the crustal thickness model from gravity inversion is very close to that of the *P* wave model [*Leinweber et al.*, 2013]. Along both profiles, the average difference in thickness of the crystalline crust is less than 2 km. More importantly, the area landward of where fracture zones terminate has crustal thickness difference of less than 1 km.
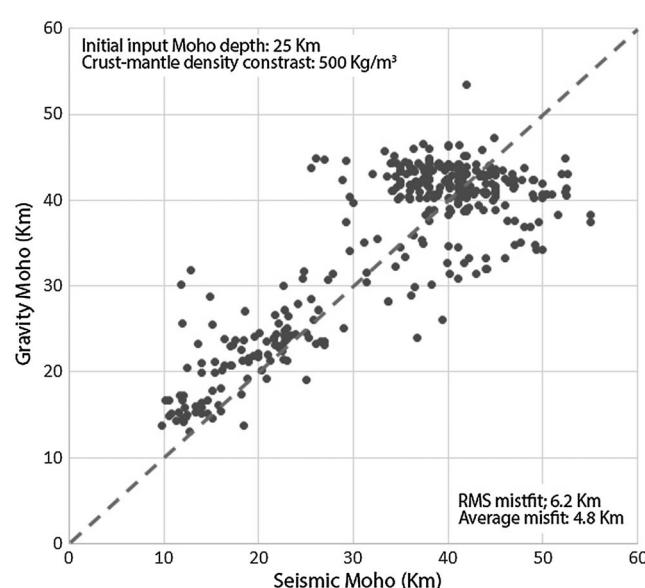
Figure 7. Correlation between depth of Moho from gravity inversion and seismic measurements. The gravity inversion uses the parameters that minimize the RMS error.

Comparisons between crustal thicknesses in the Risser Larssen Sea also yielded similar results. In profile D (Figure 10d), which trends N-S across the margin, crustal thickness from gravity inversion is generally in agreement with the ray tracing model to several hundred meters. The only noticeable differences are seen at a few narrow zones along this profile where the inverted Moho is about 2 km deeper than that of the *P* wave model. These zones are likely oceanic in nature. Profile C (Figure 10c) is in the E-W direction extending across the Astrid Ridge into the western half of the Riiser-Larsen Sea. Along this profile, crustal thickness derived from the two model types are in very good agreement with the only exception at the Astrid Ridge where ray tracing model shows Moho depth at more than 6 km shallower than the inverted Moho. One possible explanation of this discrepancy is the volcanic nature of the Astrid
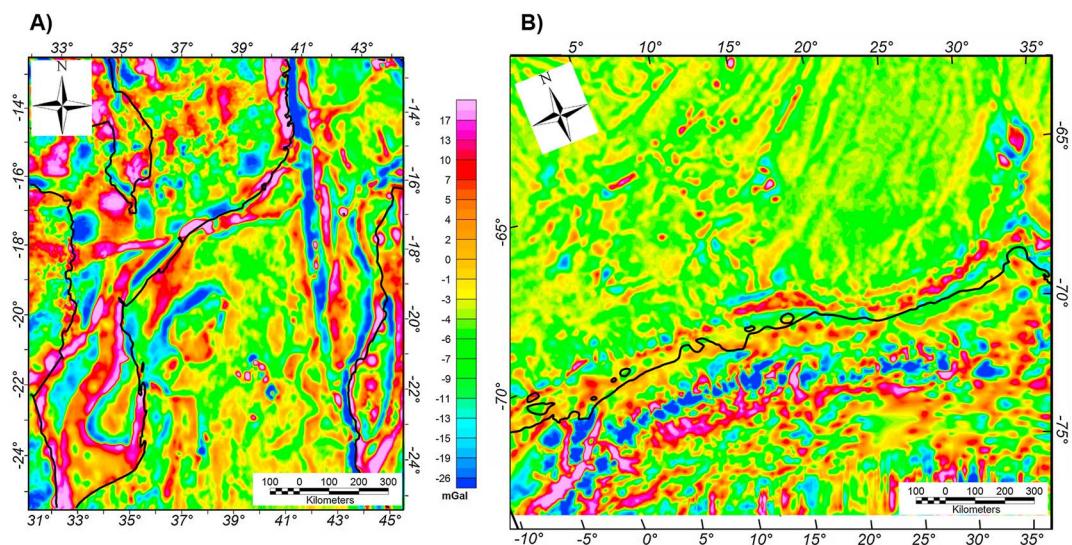
Figure 8. Difference between observed and calculated gravity anomaly (a) over the Mozambique Basin and (b) the Riiser-Larsen Sea. Map projection: Albert conic, equal area.

Ridge. The ridge might be underplated by magmatic body with density higher than the uniform 2.85 g/cc used in the gravity model. In addition, unlike the situation in the Mozambique Basin, a very thin sediment layer covers the Astrid Ridge and thus does not compensate for the increased crustal density. In such an area, the effect of crustal thinning from high density volcanic body will be accounted for during the nonrigid reconstruction stage. Nevertheless, the comparable results from the gravity model and that of other independent studies support our estimate for crustal thickness in the study areas.

3.3. Locations of the Continent-Ocean Boundaries (COBs) and Rigid Reconstruction

The magnetic anomaly map for Antarctic region [*Maus et al.*, 2007] is shown in Figure 11a. In the eastern Lazarev Sea around 67.5°S and 7°E, a NE-SW elongated positive magnetic anomaly with an average amplitude of 300 nT has been postulated as marking the COB along its northern edge [*Jokat et al.*, 2004]. Their proposed COB was supported by seismic refraction data which indicate an abrupt change in crustal thickness from 7 to 15 km over a distance of 30 km. It was also recognized that the magnetic anomaly marks the seaward extension of the seaward dipping reflector sequences (SDRs) in this area.

A similarly prominent positive magnetic anomaly is present along the Antarctica coastline over the Riiser-Larsen Sea spanning between 20–32°E and 67.5–71°S. This anomaly is in a zone where the crust thins from 42 to 7 km over a distance of 80 km. Other pieces of evidence that suggest the magnetic anomaly might be associated with the COB are the fracture zones traced from satellite-derived gravity anomalies. Figure 11a shows the fracture zones terminate against the proposed COB picked from the magnetic anomaly and crustal thickness boundary. The white dashed portion of the COB indicates area of the Astrid Ridge where the magnetic anomaly is disrupted and the trend of crustal boundary is discontinuous due to the thick volcanic emplacement that makes up the ridge.

Carrying the same analysis to the conjugate margin over the Mozambique Basin, another magnetic anomaly with similar characteristics in wavelength, amplitude, and shape is located along the Mozambique coastline in the area between 16–18°S and −36–40°E (Figure 11b). Correlation between this anomaly and the boundary of high crustal thickness gradient also yields a good match (Figure 11b). As with the COB over the Riiser-Larsen Sea, fracture zones F and G can be traced back landward until they reach the magnetic anomaly. The trend of crustal thickness and magnetic anomaly continues eastward to the Davie Fracture Zone which marks the boundary between continental Africa and oceanic crust of the Somali Basin. In contrast, the westward extension of the COB in Mozambique is not well defined. The E-W magnetic anomaly is terminated by a N-S magnetic anomaly which also marks the westward extent of the crustal thickness boundary. Locating the COB is this area is also a challenge as fracture zone E cannot be traced north of the Beira High. There is
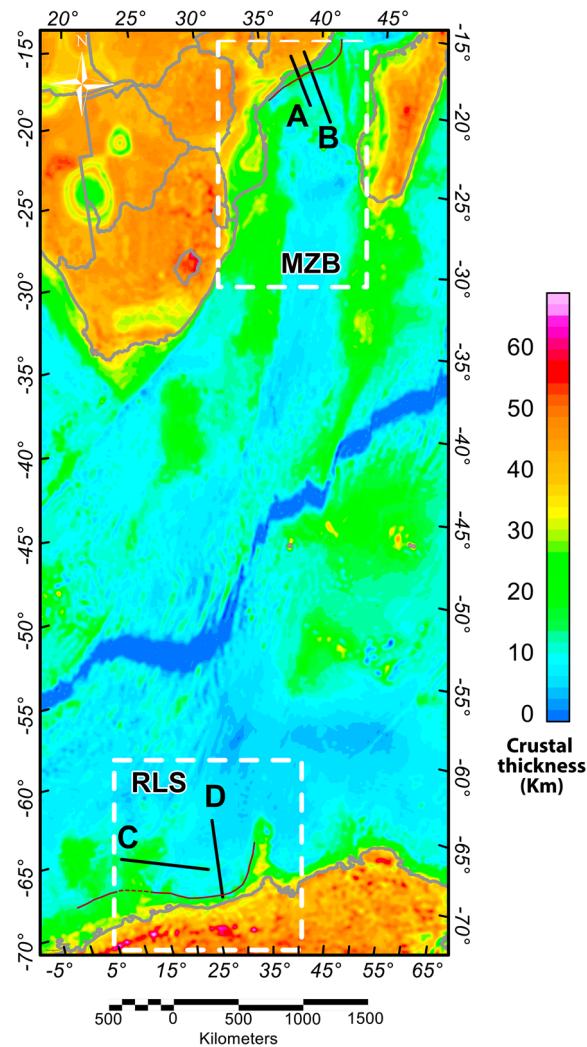
Figure 9. Thickness map of the crystalline crust calculated by subtracting the inverted Moho from the basement depth. The result is consistent with global means for thickness of continental and oceanic crusts. Continental crust is about 50 km in average. Thickness of ocean crust is in the range of 4.5–10 km. Lines A, B, C, and D in the Mozambique Basin and the Riiser-Larsen Sea are location of crustal profiles from previous studies used to evaluate the gravity inversion results. Thin brown lines mark locations of abrupt change in crustal thickness. Map projection: Albert conic, equal area.
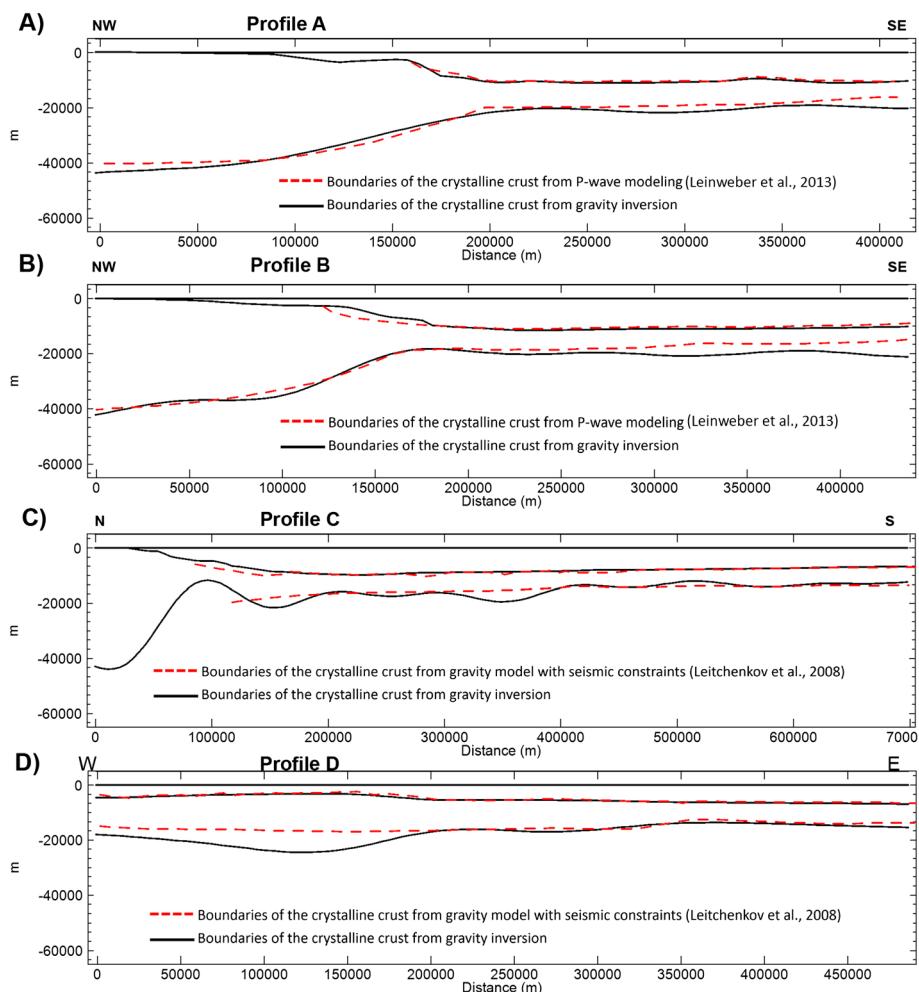
a possibility that the COB might continue southward following the crustal thickness boundary (dashed line in Figure 11b). It is also possible that the COB continues westward to another N-S oriented magnetic anomaly along 34°S even though the crustal thickness is relatively uniform over the Mozambique Coastal Plain. Nevertheless, a more complete COB over the Mozambique Basin can be determined by rigidly restoring the COB over the Riiser-Larsen Sea back to the African side.

COBs for the conjugate margins are redefined by rigid reconstruction. Magnetic anomaly picks from *Leinweber and Jokat* [2012] were used to reconstruct Antarctica during the period 124.8–149.5 Ma. While *Leinweber and Jokat* [2012] identified M41n as the oldest magnetic anomalies over the Mozambique Basin, these anomaly picks conflict with the orientation of fracture zones interpreted in this study. Our reexamination of published magnetic anomaly profiles showed that identification of anomaly in region landward of M22n1n was less reliable due to subdued anomaly amplitude. Therefore, for times older than 149.5 Ma, Antarctica is reconstructed along the identified fracture zones until the conjugate COBs come into contact. Figure 12 shows the correlation between the African and Antarctic COBs at approximately 171 Ma. The 171 Ma age is postulated based on spreading rate at 149.5 Ma (M22n1n). With the exception of the eastern and western ends, the two boundaries are generally well correlated. In the western end, the uncertainty with regard to the African COB as previously mentioned can be reduced by adopting the Antarctic COB for this part of the margin. In the eastern end, fracture zone H appears to be the conjugate of the Davie Fracture Zone (DFZ) which marks the boundary between the continental crust of Africa and oceanic crust of the West Somali Basin

[*Rabinowitz et al.*, 1983; *Gaina et al.*, 2013]. This conjugality, therefore, constrains the eastern limit of Antarctic COB to fracture zone H. The pronounced positive magnetic anomaly along the coast of Antarctica between 22°E and 35°E, which was initially interpreted as mark of the COB, could instead be evidence of magmatic intrusions onto rifted continental crust as proposed by *Leitchenkov et al.* [2008]. Figure 13 shows the consistent trend between the interpreted fracture zones and synthetic flowlines produced by rigid reconstruction.

3.4. Nonrigid Reconstruction

In a nonrigid reconstruction, it is necessary to determine the boundary between stretched and unstretched continental crust. Crustal thickness in East Antarctica is about 41 km on average [*Baranov and Morelli*, 2013], while *Tedla et al.* [2011] reported crust in the southern Africa region with 42–44 km thickness. Since our

Figure 10. (a and b) Comparisons between crustal thickness model derived from gravity inversion and seismic-constrained *P* wave model in the Mozambique Basin. The results are very comparable along Profile A. At about 200 km from the coast in Profile B, the inversion may overestimate the crustal thickness by 3–5 km. (c and d) Comparing crustal thickness derived from gravity inversion and seismic-constrained gravity model in the Riiser-Larsen Sea. Similar crustal thickness are estimated along most of Profile C except for area of the Astrid Ridge where inverted crustal thickness is greater from 1 to 6 km. Along Profile D, the results agree to a few hundred meters with only one or two locations where the difference reach maximum of 5 km.

crustal model shows that thickness of 43 km and above is relatively localized in Africa, scenario test for crustal thickness of 39, 40, 41, and 42 km was performed to determine the boundary of unstretched crust. The boundary that produced the smallest RMS misfit between the conjugate margins was used in the final model. However, the fit of nonrigid reconstruction is also dependent on the direction along which the margins are reconstructed. This study examined three different directions of extension: N-S extension, uniform WNW-ESE, and WNW-ESE with a small amount rotation (closer pole of rotation). Table 3 lists the RMS and average misfit of the restored boundaries resulting from different combinations of original crustal thickness and direction of extension. The smallest misfit is yielded by using 42 km as the prerift crustal thickness and restoring the margin in a uniform WNW-ESE direction.

Restoring the margins in a N-S direction implies continental rifting took place in a similar orientation to early seafloor rifting. Visual inspection, nevertheless, showed this scenario was not favorable as the distance between the restored boundaries of the conjugate margins significantly broadened from east to west (Figure 14). Alternatively, geological evidence suggests the Grunehogna Craton was originally connected to the Kaapvaal Province [*Groenewald et al.*, 1991; *Grantham et al.*, 2008], and part of the Explora Wedge is a conjugate feature of the Lebombo Monocline [*Cox*, 1992; *König and Jokat*, 2010]. To bring these features into proximity with each other, Antarctica was restored in a more westerly direction. Figures 15 and 16 show
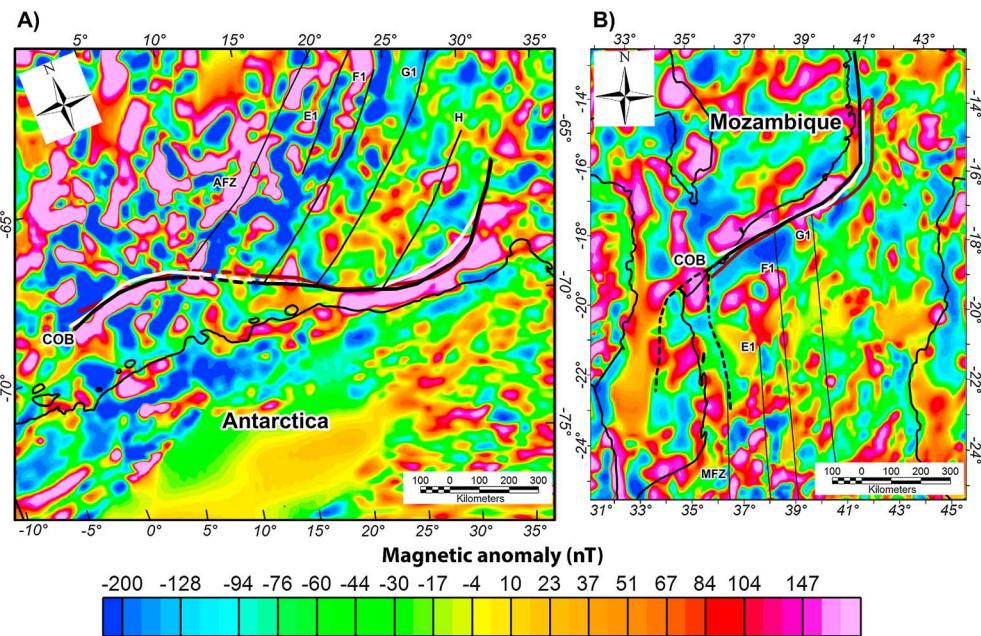
Figure 11. Reduction to the pole of the total magnetic intensity over (a) the Mozambique Basin and (b) the Riiser-Larsen Sea. Solid white lines are the seaward edge of the pronounced positive anomalies. Solid grey lines represent locations where crustal thickness changes abruptly (Figure 4). Note how the grey and white lines are closely correlated spatially with each other and with the termination of the fracture zones in the conjugate margins. The picked COBs are shown as solid black lines. Map projection: Albert conic, equal area.

more consistent trends between the African and Antarctic restored boundaries when reconstructed in either a uniform WNW-ESE or curved WNW-ESE direction.

Seismic refraction data from *Leinweber et al.* [2013] show the presence of high velocity lower crustal body in the Mozambique continental margin that was interpreted as magmatic underplating. The interpretation from *Leinweber et al.* [2013] indicated that the underplate had a maximum lateral extent of 100 km landward from
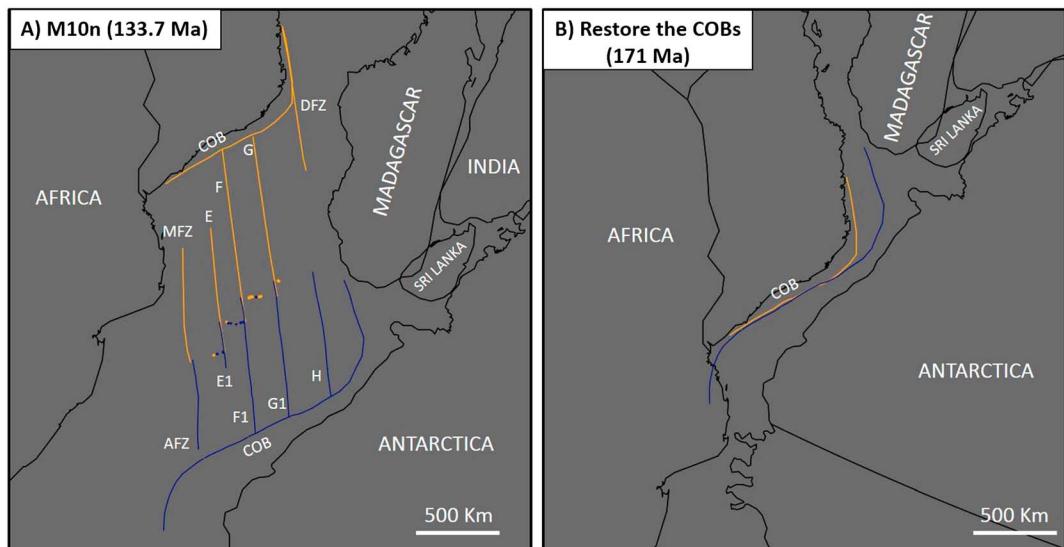
Figure 12. (a) Plate reconstruction at 133.7 Ma shows the correlation between the African fracture zones (yellow line) and theirs conjugates from Antarctica (blue lines). Small dots are identified magnetic anomalies M10n from the Mozambique Basin (yellow) and the Riiser-Larsen Sea (blue). Note the correlation between fracture zone H and the Davie Fracture Zone (DFZ). (b) Reconstruction at 171 Ma when the conjugate COBs are restored. Significant misfit exists in the eastern end of the COBs where the Antarctic boundary is place over crust that has previously been considered oceanic.
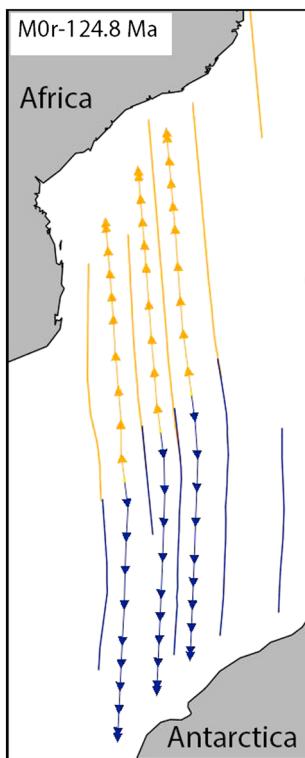
Figure 13. Reconstruction map at M0r showing the correlation between interpreted fracture zones (solid lines) and the synthetic flowline (lines with arrows) generated from the model. African features are shown in yellow. Antarctic features are shown in blue.

interpreted COB. The volume of underplate calculated from these interpretations averages to be approximately 6.5 km in thickness. Based on seismic reflection data across the Zambezi Delta and Beira High area, lavas flow thickness is estimated to be about 3–5 km [*Mahanjane*, 2012]. The calculated thickness of related mafic material at the base of the crust would equate to a 7.5–12.5 km of underplate, using the relationship derived in Table 1. To account for mafic underplating along the profiles, the inverted Moho must be corrected. Such correction is calculated based on isostasy and the density contrast between the crystalline crust (2.85 g/cc), magmatic underplating (3.05 g/cc), and upper mantle (3.3 g/cc). A simple isostatic equation gives $x*(3.05–2.85) = (1 − x)*(3.3–3.05)$ where x is the amount (in kilometer) the crust thins for each kilometer in thickness of added underplating, x is estimated to be 0.55 km. For example, in a simplified end-member model, assuming uniform and maximum underplate thickness of 12.5 km across an area of 100 km landward of the interpreted COB would result in a 6.87 km thinner crust compared to the inversion result. Using the corrected crustal thickness as described above, we restored the extended continental crust along all extracted 2-D profiles. Figures 15 and 16 reflect the reconstructions that account for both volcanic and nonvolcanic margins.

Reconstruction geometries and correlations of prerift boundaries from the conjugate, volcanic margins are shown in Figures 17 and 18. Assuming continental rifting took place along a uniform WNW-ESE direction produces a tighter fit for Africa and Antarctica, Africa and Madagascar, as well as between Africa and India. The Lebombo Monocline and the Kappvaal Province are reconstructed to their proposed conjugates: the Explora Wedge and Grunehogna Craton, respectively. Timing of the nonrigid closure is taken to be 184 Ma coeval with the eruption of Karoo flood basalt [*Duncan et al.*, 1997].

Figure 19 shows the correlation of magnetic anomaly from Africa and Antarctica in the full-fit reconstruction. Similar magnetic characters (wavelengths and amplitudes) are observed between the Kaapvaal Province and the Grunehogna Craton. Likewise, magnetic anomalies over the Mozambique Province and the Central Dronning Maud Land also express similar patterns.

Since the final model, which describes the initial motion of Antarctica as a WNW-ESE rift from Africa, generates a consistent match of the restored boundaries without any major overlap or gap in the reconstruction and effectively brings back geological features that are conjugate, it is considered to be the preferred model of this study. Table 4 lists the calculated poles of rotation for the reconstruction of Antarctica with respect to Africa from 124.8 Ma (M0r) to 184 Ma (full fit).

Table 3. Scenario Test to Determine the Unstretched Crustal Thickness and the Direction of Continental Extension[a]

| Direction of Extension	Uniform WNW-ESE				Curved WNW-ESE			
Prerift thickness	39 km	40 km	41 km	42 km	39 km	40 km	41 km	42 km
RMS misfit	23.4 km	21.7 km	22.1 km	16.8 km	23.8 km	23.3 km	22.5 km	22.3 km
Average misfit	18.1 km	17.1 km	16.3 km	12.5 km	16.0 km	17.1 km	15.9 km	15.6 km

[a]Using a prerift thickness of 42 km and restoring Antarctica in a uniform WNW-ESE direction yield the lowest RMS and average misfits between African and Antarctic restored boundaries along 19 extracted 2-D profiles.
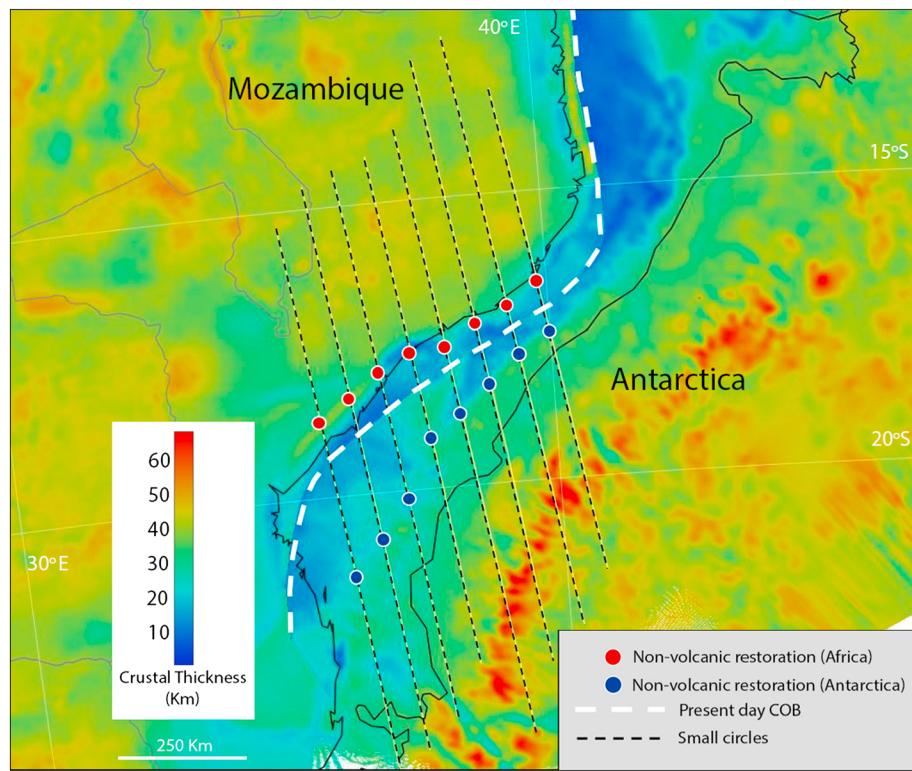
Figure 14. Reconstruction map at 171 Ma (rigid fit) illustrates the extraction of 2-D profiles across the Africa and Antarctica conjugate margins in a roughly N-S direction. On either margin, each profile is extended from the present-day COB landward to the boundary of 42 km crustal thickness. Red dots represent restored prerift boundary on the African side, and blue dots are the Antarctic counterparts. Note that from east to west, the distance between the restored boundaries widens progressively indicating a bad nonrigid fit.
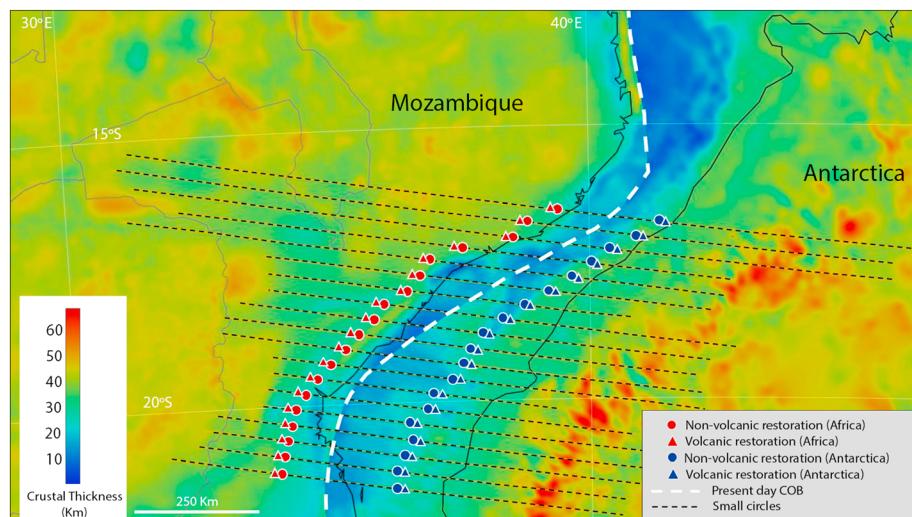
Figure 15. Reconstruction map at 171 Ma (rigid fit) illustrates the extraction of 2-D profiles across the Africa and Antarctica conjugate margins in a uniform WNW-ESE direction. On either margin, each profile is extended from the present-day COB landward to the boundary of 42 km crustal thickness. Red dots represent restored prerift boundary on the African side and blue dots are the Antarctic counterparts. Triangles mark the restored boundaries after subtracting area of magmatic underplating along each profile. Note that restoring the margins in this direction, as opposed to N-S, produces a much more consistent trend of the restored boundaries.
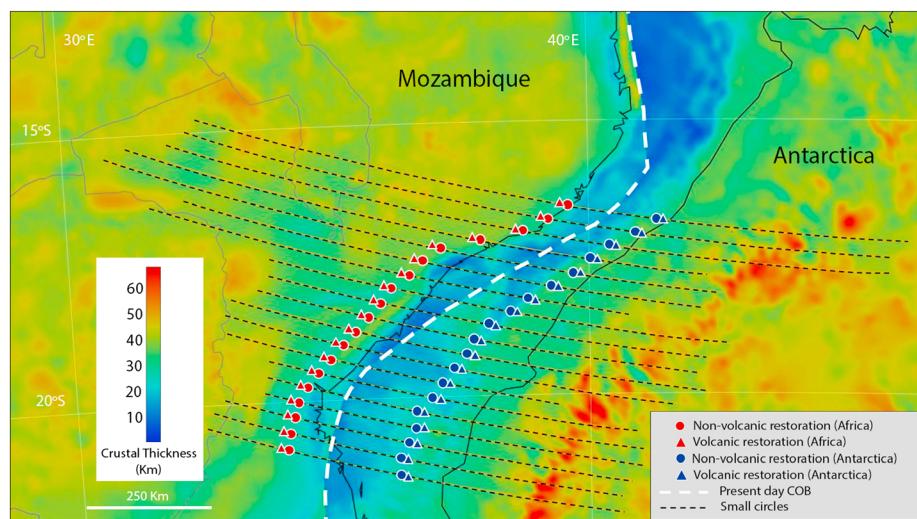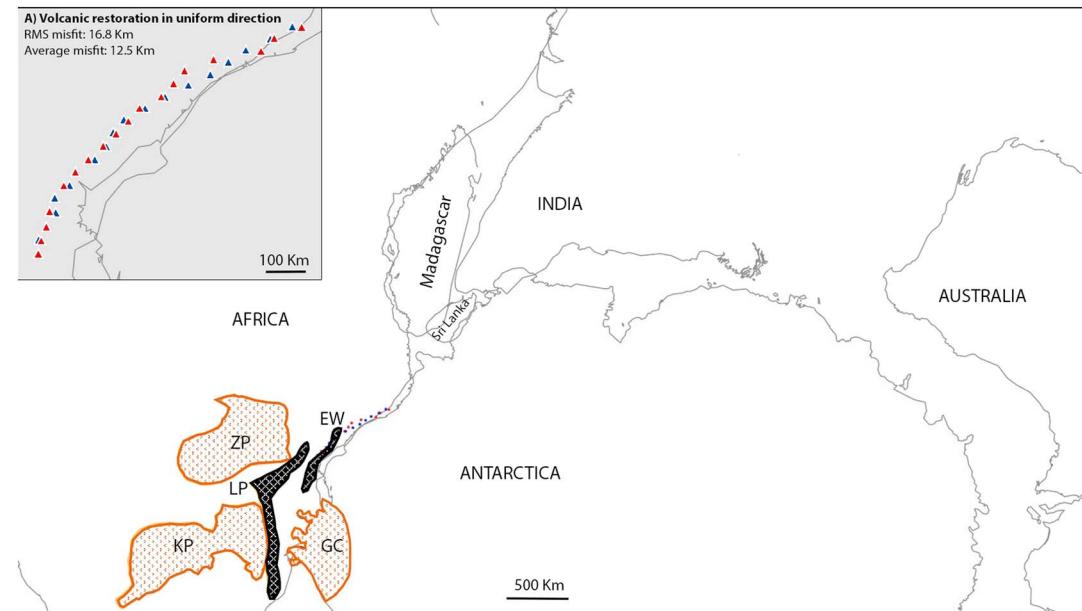
Figure 16. Reconstruction map at 171 Ma (rigid fit) illustrates the extraction of 2-D profiles across the Africa and Antarctica conjugate margins in curved WNW-ESE direction. On either margin, each profile is extended from the present-day COB landward to the boundary of 42 km crustal thickness. Red dots represent restored prerift boundary on the African side and blue dots are the Antarctic counterparts. Triangles mark the restored boundaries after subtracting area of magmatic underplating along each profile. Note that restoring the margins in this direction, as opposed to N-S, produces a much more consistent trend of the restored boundaries.

4. Discussion

4.1. Initial Crustal Thickness

In the nonrigid restoration presented here, an assumption is made regarding the initial thickness of undeformed continental crust. Reported crustal thicknesses for Antarctica vary considerably from less than 30 km beneath the Filchner-Ronne Ice Shelf to more than 56 km in the region of the Gamburtsev Subglacial Mountains of East Antarctica [*Baranov and Morelli*, 2013]. More specifically, Antarctic crustal

Figure 17. Reconstruction map showing East Gondwana prerift fit at 184 Ma. From their rigid fit location at 171 Ma, Antarctica, Madagascar, India, Sri Lanka, and Australia are moved together in a uniform WNW-ESE direction toward Africa. This reconstruction accounts for added magmatism during rifting. Inlet map shows the correlation between African and Antarctic restored boundaries. Red and blue triangles are volcanic restored point on the African and Antarctic sides, respectively.
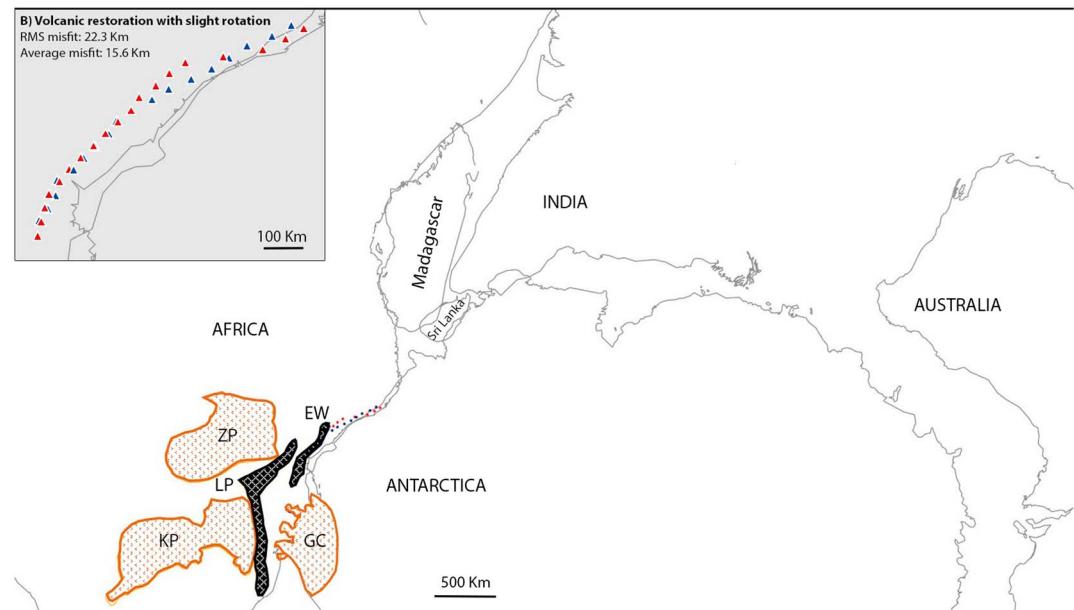
Figure 18. Reconstruction map showing East Gondwana prerift fit at 184 Ma. From their rigid fit location at 171 Ma, Antarctica, Madagascar, India, Sri Lanka, and Australia are rotated together in a slightly curved WNW-ESE path toward Africa. This reconstruction accounts for added magmatism during rifting. Inlet map shows the correlation between African and Antarctic restored boundaries. Red and blue triangles are volcanic restored point on the African and Antarctic sides, respectively. Note the higher RMS misfit and a less tight fit of Antarctica, Madagascar, and India to Africa compared to Figure 17.
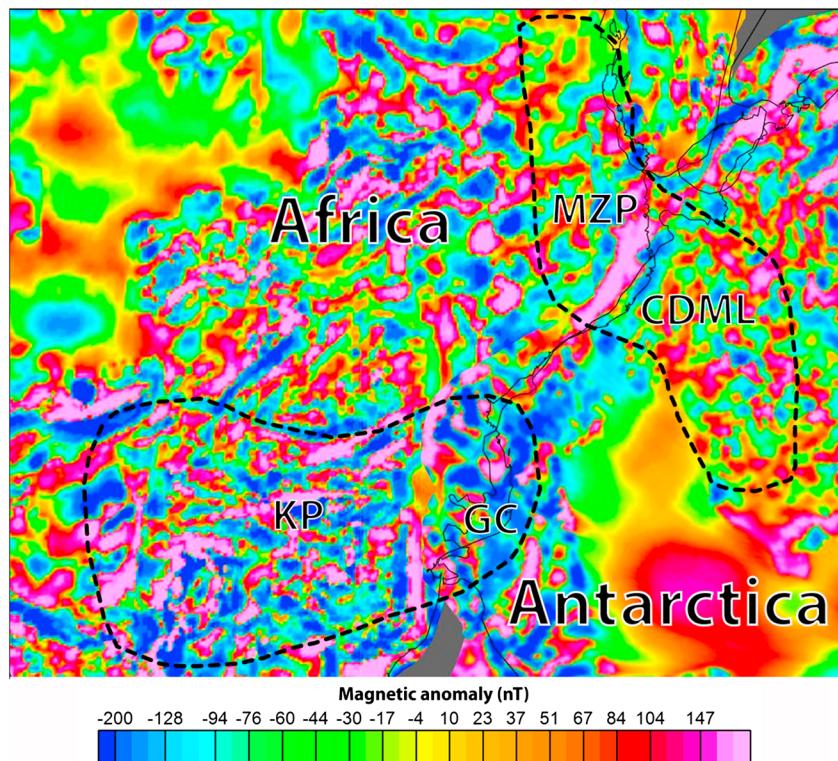
Figure 19. Correlation of the magnetic anomalies over Africa and Antarctica in their original position as restored by nonrigid reconstruction. Dashed outlines are regions that express magnetic anomalies of similar wavelengths and amplitudes. KP: Kaapvaal Province, GC: Grunehogna Craton, MZP: Mozambique Province, and CDML: Central Dronning Maud Land. Map overlay is reduction to the pole of the total intensity magnetic anomaly [*Maus et al.*, 2007].

Table 4. Poles of Rotation for the Reconstruction of Antarctica With Respect to Africa[a]

Magnetic Anomaly	Time (Ma)	Latitude	Longitude	Angle (deg)
M0r	124.81	−12.75	−24.05	43.89
M3n	127.86	−12.71	−24.46	44.78
M5n	130.28	−12.55	−24.84	45.67
M5r	131	−13.04	−24.4	46.28
M6n	131.3	−13.1	−24.44	46.57
M7r	132.03	−12.97	−24.62	46.67
M8n	132.36	−13.1	−24.53	46.92
M8r	132.68	−12.9	−24.75	46.88
M9n	132.99	−13.43	−24.26	47.41
M9r	133.32	−14.31	−23.38	48.19
M10n	133.69	−14.91	−22.81	48.82
M10r	134.09	−15.61	-22.09	49.54
M10Nn2n	134.83	−16.39	−21.24	50.51
M10Nr	135.49	−16.47	−21.26	50.83
M11r2r	136.81	−16.45	−21.32	51.58
M12n	137.71	−16.17	−21.63	51.67
M15n	140.51	−15.25	−22.66	52.11
M15r	140.86	−15.18	−22.75	52.16
M18r	144.73	−14.14	−23.97	53.23
M19n2n	145.51	−14.51	−23.61	53.97
M19r	146.06	−14.78	−23.32	54.39
M20n1n	146.32	−14.47	−23.7	54.41
M20r	147.47	−14.26	−23.96	54.58
M21n	148.16	−14.46	−23.74	54.91
M21r	148.73	−14.57	−23.65	55.32
M22n1n	149.49	−14.11	−24.16	55.6
Rigid Fit	171	−12.52	−26.2	60.85
Full Fit	184	−13.72	−28.25	61.19

[a]Magnetic reversal timescale is adopted from *Gradstein et al.* [2004].

thicknesses onshore of the Africa-Antarctic corridor in this study are generally between 34 and 48 km with an average value close that of East Antarctica (viz., 41 km) [*Baranov and Morelli*, 2013]. Crustal thicknesses reported for southern Africa are typically 42–44 km [*Tedla et al.*, 2011]. The method used here restores both margins to the same prerift thickness. This is justified by assuming a gradual change in thickness over Gondwana, and that, where initial rifting took place, the crust had the same thickness on either side of the rift.

Although our test indicated using 42 km as initial crustal thickness produced a lowest misfit, we have examined the effects of using different thicknesses of 39, 40, and 41 km on the final fit of the restored boundaries. These values are comparable to the average crustal thickness of Africa and Antarctica as reported by independent seismic studies. Our test showed that while varying the prerift thickness from 39 to 42 km results in different locations of the restored COB, the overall shape of these boundaries did not vary significantly. Moreover, the maximum distance between a restored COB from using 39 km prerift thickness and that from using 42 km is less than 30 km. Therefore, the uncertainty in our model due to initial prerift thickness is in the order of a few tens of kilometer.

4.2. Volcanic Margins

The nature of the margins, whether volcanic or nonvolcanic, together with uncertainties attached to estimating total volcanic volume influences the crustal thickness that must be accommodated in any nonrigid reconstruction. Here we assume that both margins are volcanic, and that the plates underwent pure shear rifting [*McKenzie*, 1978] producing magmatic underplating beneath each margin. It is also assumed that there is a relationship between SDR thickness and the amount of magmatic underplating beneath a volcanic margin. Although we have examined several volcanic margins to estimate these amounts, insufficient data are currently available to establish a strong correlation between them. In contrast, there is some limited evidence from the southwest African margin that the ratio of SDRs to underplating may vary along strike [*Trumbull et al.*, 2007; *Hirsch et al.*, 2009], although this has not been documented along the Mozambique or Antarctica margin.

Most evidence for magmatic underplating is found on the African side. Limited data from Antarctica have not suggested the significant presence of magmatic underplating in the Riiser-Larsen Sea region [*Leitchenkov et al.*, 2008; *Hinz et al.*, 2004]. However, there is evidence of syn-tectonic volcanism in the Riiser-Larsen shelf area [*Leitchenkov et al.*, 2008; *Kristoffersen et al.*, 2000]. If the Antarctic margin is nonvolcanic, then its nonrigid restoration could be less and its prerift boundary would be moved up to ~ 15 km outboard of the calculated volcanic prerift boundary as shown in Figure 15. While there are uncertainties relating to the true lateral extent of underplated material cross the Mozambique and Antarctic margins, the correction is relatively small on all our reconstructed profiles and consequently Antarctica would simply be moved away from Africa by a few tens of kilometers resulting in a less tight fit. Interestingly, should our model be underestimating the amount of underplating in the SW region of the Mozambique Basin (i.e., the Mozambique Coastal Plain region) farther landward correction of the prerift boundary would result in greater rotation of Antarctica toward Mozambique. This, however, would cause significant space problems between Madagascar and East Africa in the present model. Similarly, an overestimation of the magmatic underplate in the NE region of Mozambique would yield similar problems. Our maximum assumption of the underplate thickness is 6.0 km greater than that reported by *Leinweber et al.* [2013], this will only modify our prerift boundary by the order of a few kilometers.
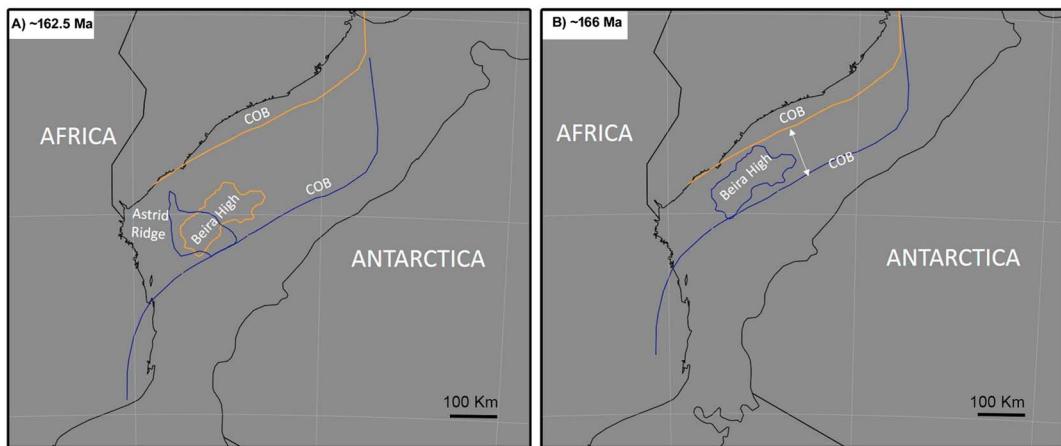
4.3. Beira High

Based upon seismic reflection data, *Mahanjane* [2012] interprets the Beira High to be a continental block with abrupt boundaries where the ocean-continent transition occurs in a 5–10 km wide zone. Continental basement is identified at ~ 5 s two-way-traveltime [*Mahanjane*, 2012] suggesting a depth of ~6–7 km. Our inverse gravity model indicates an average crustal thickness of 19 km for the Beira High, which is consistent with it being either a continental fragment or an oceanic plateau [*Tetreault and Buiter*, 2014]. Unfortunately, the only seismic refraction data collected over the Beira High could not provide velocities of its lower crust without ambiguity due to a sparse ray coverage [*Mueller et al.*, 2015]. Velocity information for the lower crustal layers might prove more diagnostic of its deep structure.

To accommodate a continental Beira High in their reconstruction model, *Leinweber and Jokat* [2012] propose a short-lived spreading center between the Beira High and Africa that was active from 167 Ma to 159 Ma after which spreading jumped to the southern margin of the Beira High. However, no symmetric pattern of magnetic isochrons has been mapped to support this early spreading. The presence of oceanic crust directly north of the Beira High is supported by our crustal thickness model (Figure 9), which shows a 115–120 km wide zone between the Beira High and the Africa COB with crustal thicknesses that range from 4.5 to 10 km, similar to that of the ocean basin to the east. In our reconstruction, the Antarctica COB comes into contact with the southern margin of the Beira High at 162.5 Ma, at which point the ocean basin width to the east is roughly twice that of the basin immediately north of the Beira High. If we position the Beira High against the African COB at ~ 166 Ma, there is still 115 km of oceanic crust on its eastern side (Figure 20). One way to accommodate this discrepancy would be with two basins, one north and one east of the Beira High, that open simultaneously but at substantially different rates. This would require that between 166 and 162.5 Ma Antarctica rotates clockwise about a pole of rotation sufficiently close to produce a large difference in spreading over a relatively short distance. Such a pole would produce strongly curved fracture zones, which are inconsistent with the observed fracture zone traces that show continuous, linear N-S trends.

An alternative way to resolve the issue of the overlap introduced by a continental Beira High is to move the COBs for Africa or Antarctic (or both) farther landward by a combined 110 to 120 km. The location of the Antarctica COB between 9°E and 15°E is well supported by geophysical data including the truncation of FZ traces, the associated change in crustal thickness, and the boundary parallel magnetic anomaly. East of 37°E the Africa COB is also well defined by geophysical data but farther west, in the vicinity of the Beira High, the COB is less well constrained. For example, fracture zone E cannot be followed north of the Beira High. However, the boundary parallel magnetic anomaly appears continuous across the area, and our crustal model does not show any appreciable northward (i.e., landward) step in crustal thickness variations. It appears that a more northerly Africa COB while possible does not correlate as well with available geophysical data.

Finally, if the Beira High is a 19 km thick, continental fragment with widespread volcanism [*Mahanjane*, 2012], then restoring it to an initial 42 km thickness would reduce its N-S extent from 115 km to < 50 km producing a corresponding 50 km overlap in our nonrigid reconstruction.

Figure 20. Reconstruction map at (a) 162 Ma when the southern Astrid Ridge overlapped the Beira High suggesting they are conjugate features. During this time the Antarctic COB also came into contact with the Beira High. Note the area of oceanic crust east of the Beira High is significantly wider than area to its northwest. (b) Assuming the Beira High is a continental fragment that was attached to Antarctica prior to 162 Ma, at 166 Ma the ocean basin between the high and Africa was closed but 115 km of oceanic crust still existed east of the Beira High.

4.4. Areas for Further Research

Many plate models including the interpretations here rely heavily on the interpretation of a COB and the understanding of the distribution of crustal thinning across Mozambique and Antarctica. In our preferred model there remains uncertainty in the COB location along the Mozambique Coastal Plain. Currently, we do not have any high-quality seismic data to provide constraints on the nature of the crust in this region. Additional seismic data would also assist in mapping the extent of volcanics and possible underplate across the margins.

Another key uncertainty within our model and other full-fit plate models is the assumed age of the full fit. The age of breakup and seafloor spreading is not well delineated due to limited magnetic data in the public domain. Similarly, the initiation of rifting is poorly constrained. It is not well constrained what the initiation age of rifting is in Mozambique or Antarctica. In our model we assume an age of 184 Ma, whereas *Reeves and de Wit* [2000] assumed 200 Ma to be a prerift fit. A better understanding of rift age versus Karoo volcanism would help improve the rift kinematics assumed in this model; our current model assumed that rift initiation and major period of Karoo volcanics are coeval.

Finally, observations from *Mahanjane* [2012], *Flores* [1973], *Kamen-Kaye* [1983], *Kristoffersen et al.* [2000], *Segev* [2002], and *König and Jokat* [2010] suggest Karoo magmatism continued in the region between ~204 and 140 Ma. It is possible, therefore, that the Mozambique Coastal Plain is in fact thickened oceanic crust as predicted in our model and that of *Eagles and König* [2008] and *Marks and Tikku* [2001]. The thickened corridor of oceanic crust in the SW region here perhaps implies that there was a strong interplay between the large magma budgets and early seafloor spreading in the SW region of Mozambique. Further research is needed to determine whether the presence of thickened magmatic crust is related to the continued influence of the Karoo plume or some other mechanisms.

5. Conclusions

Gravity anomaly data reveal fracture zones that can be traced as far landward as 70 km off African and Antarctic coastlines. The Mozambique Basin is separated into at least four spreading corridors. Likewise, the five fracture zones are identified over the Riiser-Larsen Sea which are determined to be conjugates of the fracture zones over the Mozambique Basin.

Three-dimensional gravity inversion has produced a crustal thickness model that shows onshore Africa and Antarctica have average crustal thickness of 40 km and 55 km, respectively. The oceanic crust over the Mozambique Basin and the Riiser-Larsen Sea has thickness ranging from 4 to 10 km. Analyses of magnetic
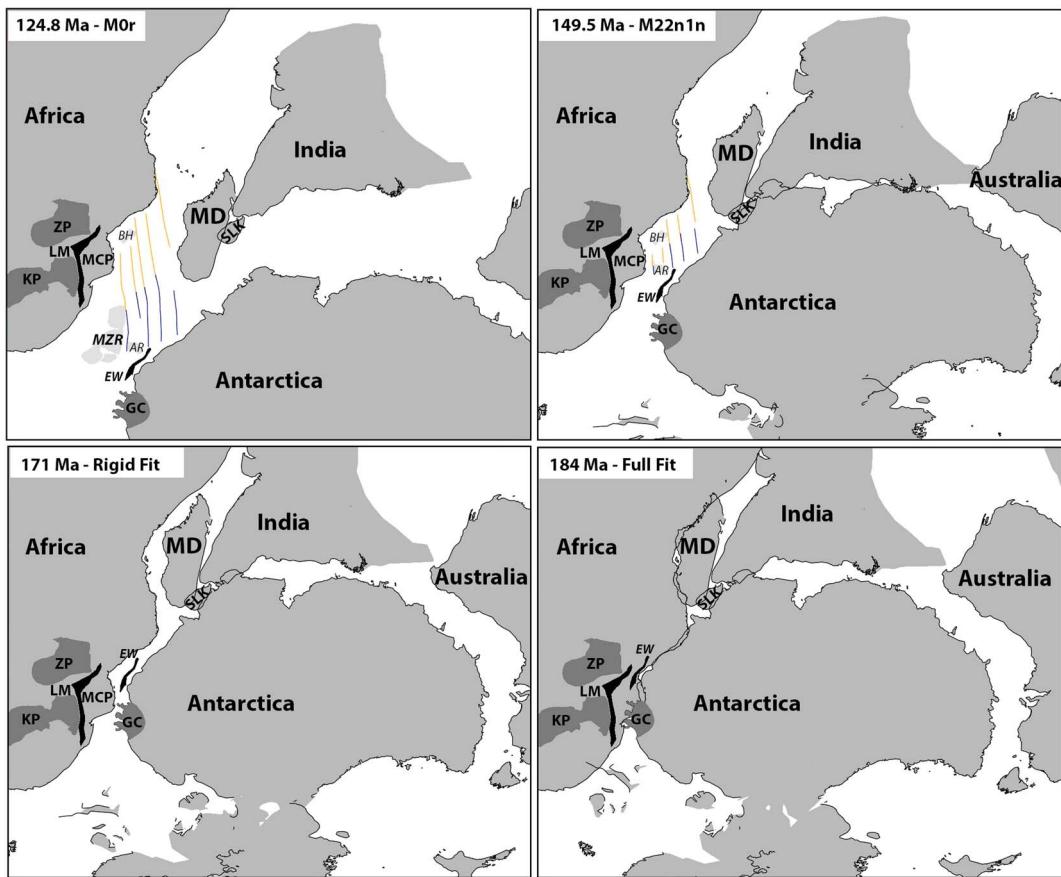
Figure 21. Plate reconstructions showing the evolution of the continental margin of Africa along the Mozambique Basin and its conjugate Antarctic margin over the Riiser-Larsen Sea. Reconstruction poles for Madagascar, India, and Sri Lanka prior to 170 Ma are from *Gaina et al.* [2015]. Other plates are from *Seton et al.* [2012]. Italic letters indicate submarine structures. Dark grey are cratonic terranes. AR: Astrid Ridge, BH: Beira High, EW: Explora Wedge, GC: Grunehogna Craton, KP: Kaapvaal Province, LM: Lebombo Monocline, MCP: Mozambique Coastal Plain, MD: Madagascar, MZR: Mozambique Ridge, SLK: Sri Lanka, and ZP: Zimbabwe Province. Yellow and blue lines are fracture zones on the African and Antarctic sides, correspondingly.

anomalies and crustal thickness along with identified fracture zones reveal the COBs that are located significantly closer to the coasts of Africa and Antarctica than previously recognized.

The conjugate margins of Africa and Antarctica are reconstructed by correlating fracture zone azimuths together with the identified COBs. The results show early plate motion was in a N-S direction with Antarctica drifted southwardly with respect to Africa. Of several scenarios examined to determine the crustal character of the Beira High, the preferred model assigns it an oceanic origin and suggests that it may be a conjugate feature of the southern Astrid Ridge emplaced between 162 and 158 Ma.

An areal-balancing method that involves restoring the crust to a uniform prerift thickness has been used to perform the nonrigid reconstruction. This restoration has been carried out for both nonvolcanic and volcanic margins with magmatic underplating. Based upon the results, Africa underwent extension of 60–120 km while Antarctic crust was stretched by 105–180 km. Various models tested to determine the direction of extension during rifting suggest that Antarctica moved away from Africa in a WNW-ESE direction during the period between 184 and 171 Ma prior to the onset of seafloor spreading. In the final fit of the continents, the Grunehogna Craton occupies the present area of the Mozambique Coastal Plain and part of the Explora Wedge is placed adjacent to the Lebombo and Mateke-Sabi monoclines. Figure 21 summarizes our reconstruction model for the plate motions between Antarctica and Africa using the magnetic isochrons from *Leinweber and Jokat* [2012] and our determined fracture zones and COBs.

References

Austin, J. A., P. L. Stoffa, J. D. Phillips, J. Oh, D. S. Sawyer, G. M. Purdy, E. Reiter, and J. Makris (1990), Crustal structure of the Southeast Georgia Embayment-Carolina Trough: Preliminary results of a composite seismic image of a continental suture (?) and a volcanic passive margin, *Geology*, *18*(10), 1023–1027, doi:10.1130/0091-7613(1990)018<1023:CSOTSG>2.3.CO;2.

Bai, Y., S. Wu, Z. Liu, R. D. Muller, and S. E. Williams (2015), Full-fit reconstruction of the South China Sea conjugate margins, *Tectonophysics*, *661*, 121–135.

Baier, B., H. Beckhemer, D. Gajewski, R. W. Green, C. Grimsel, and C. Prodehl (1983), Deep seismic sounding in the area of the Damara Orogen, Namibia, Southwest Africa, in *Intracontinental Fold Belts: Case Studies in the Variscan Belt and in the Damara Belt in Namibia*, edited by H. Marin and F. W. Eder, pp. 885–900, Springer, Berlin.

Baranov, A., and A. Morelli (2013), The Moho depth map of the Antarctica region, *Tectonophysics*, *609*, 299–313, doi:10.1016/j.tecto.2012.12.023.

Barret, D. M. (1977), Agulhas Plateau off southern Africa: A geophysical study, *Geol. Soc. Am. Bull.*, *88*(6), 749–763.

Bauer, K., S. Neben, B. Schreckenberger, R. Emmermann, K. Hinz, N. Fechner, and K. Weber (2000), Deep structure of the Namibia continental margin as derived from integrated geophysical studies, *J. Geophys. Res.*, *105*, 25,829–25,853, doi:10.1029/2000JB900227.

Ben-Avraham, Z., C. J. H. Hartnady, and A. P. le Roex (1995), Neotectonic activity on continental fragments in the Southwest Indian Ocean: Agulhas Plateau and Mozambique Ridge, *J. Geophys. Res.*, *100*, 6199–6211, doi:10.1029/94JB02881.

Bentley, C. R. (1991), Configuration and structure of the subglacial crust, in *The Geology of Antarctica*, edited by R. J. Tingey, pp. 335–364, Oxford Univ. Press, Oxford.

Bergh, H. W. (1977), Mesozoic sea floor off Dronning Maud land, Antarctica, *Nature*, *269*, 686–687.

Bergh, H. W. (1987), Underlying fracture zone nature of Astrid Ridge off Antarctica's Queen Maud Land, *J. Geophys. Res.*, *92*, 475–484, doi:10.1029/JB092iB01p00475.

Bertill, D., and J. M. Regnoult (1998), Seismotectonics of Madagascar, *Tectonophysics*, *294*(1–2), 57–74, doi:10.1016/S0040-1951(98)00088-2.

Blakely, R. J. (1995), *Potential Theory in Gravity and Magnetic Applications*, Cambridge Univ. Press, New York.

Bloch, S., A. L. Hales, and M. Landisman (1969), Velocities in the crust and upper mantle of southern Africa from multi-mode surface wave dispersion, *Seismol. Soc. Am. Bull.*, *59*, 1599–1629.

Buyl, M. D., and G. Flores (1986), Southern Mozambique Basin: Most promising hydrocarbon province offshore East Africa, *AAPG Bull.*, *68*, 399–425, doi:10.1306/AD461719-16F7-11D7-8645000102C1865D.

Chave, A. D. (1979), Lithospheric structure of the Walvis Ridge from Rayleigh wave dispersion, *J. Geophys. Res.*, *87*, 6840–6848, doi:10.1029/JB084iB12p06840.

Chetty, P., and R. W. E. Green (1977), Seismic refraction observations in the Transkei Basin and adjacent areas, *Mar. Geophys. Res.*, *3*, 197–208.

Cox, K. (1992), Karoo igneous activity, and the early stages of the break-up of Gondwanaland, in *Magmatism and the Causes of Continental Break-Up*, edited by B. C. Storey, T. Alabaster, and R. J. Pankhurst, pp. 137–148, Geol. Soc. Spec. Publ., London.

Duncan, R. A., P. R. Hooper, J. Rehacek, J. S. Marsh, and A. R. Duncan (1997), The timing and duration of the Karoo igneous event, southern Gondwana, *J. Geophys. Res.*, *102*, 18,127–18,138, doi:10.1029/97JB00972.

Durrheim, R. J., W. H. Barker, and R. W. E. Green (1992), Seismic studies in the Limpopo belt, *Precambrian Res.*, *55*, 187–200.

Eagles, G., and M. König (2008), A model of plate kinematics in Gondwana breakup, *Geophys. J. Int.*, *173*(2), 703–717, doi:10.1111/j.1365-246X.2008.03753.x.

Encarnación, J., T. H. Fleming, D. H. Elliot, and H. V. Eales (1996), Synchronous emplacement of Ferrar and Karoo dolerites and the early breakup of Gondwana, *Geology*, *24*(6), 535–538, doi:10.1130/0091-7613(1996)024<0535:SEOFAK>2.3.CO;2.

Flores, G. (1973), The Cretaceous and Tertiary sedimentary basins of Mozambique and Zululand, *Assoc. Serv. Geol. Afr*, 81–111.

Fourno, J. P. (1987), Contribution a l'etude de la discontinuite de Mohorovicic d'apres les ondes sismiques observees a Madagascar Annales, *Geophysicae*, *2*, 175–186.

Gaina, C., T. H. Torsvik, D. J. J. van Hinsbergen, S. Medvedev, S. C. Werner, and C. Labails (2013), The African Plate: A history of oceanic crust accretion and subduction since the Jurassic, *Tectonophysics*, *604*, 4–25.

Gaina, C., D. J. D. van Hinsbergen, and W. Spakman (2015), Tectonic interactions between India and Arabia since the Jurassic reconstructed from marine geophysics, ophiolite geology, and seismic tomography, *Tectonics*, *34*, 875–906, doi:10.1002/2014TC003780.

Gohl, K., and N. Uenzelmann-Neben (2001), The crustal role of the Agulhas Plateau, southwest Indian Ocean: Evidence from seismic profiling, *Geophys. J. Int.*, *144*(3), 632–646, doi:10.1046/j.1365-246x.2001.01368.x.

Gore, J., D. E. James, T. G. Zengeni, and O. Gwavana (2009), Crustal structure of the Zimbabwe Craton and the Limpopo belt of Southern Africa: A new constraints from seismic data and implications for its evolution, *South African J. Geol.*, *112*(3-4), 213–228, doi:10.2113/gssajg.112.3-4.213.

Goslin, J., M. Recq, and R. Schilch (1981), Structure profonde du plateau de Madagascar-Relations avec le plateau de Crozet, *Tectonophysics*, *76*, 75–97.

Gradstein, F. M., J. G. Ogg, A. G. Smith, W. Bleeker, and L. J. Lourens (2004), A new geologic time scale, with special reference to Precambrian and Neogene, *Episodes*, *27*(2), 83–100.

Grantham, G. H., P. H. Macey, B. A. Ingram, M. P. Roberts, R. A. Armstrong, T. Hokada, and V. Manhica (2008), *Terrane Correlation Between Antarctica, Mozambique and Sri Lanka: Comparisons of Geochronology, Lithology, Structure and Metamorphism and Possible Implications for the Geology of Southern Africa and Antarctica*, vol. 308, pp. 91–119, Geol. Soc. London Spec. Publ., doi:10.1144/SP308.4.

Green, R. W. E., and A. L. Hales (1966), Seismic refraction measurements in the southwestern Indian Ocean, *J. Geophys. Res.*, *71*, 1637–1647, doi:10.1029/JZ071i006p01637.

Green, R. W. E., and R. J. Durrheim (1990), Seismic refraction investigation of the Namaqualand metamorphic complex, South Africa, *J. Geophys. Res.*, *95*, 19,927–19,932, doi:10.1029/JB095iB12p19927.

Groenewald, P. B., G. H. Grantham, and M. K. Watkeys (1991), Geological evidence for a Proterozoic to Mesozoic link between southeastern Africa and Dronning Maud Land, Antarctica, *J. Geol. Soc.*, *148*(6), 1115–1123, doi:10.1144/gsjgs.148.6.1115.

Hales, A. L., and J. B. Nation (1972), A crustal structure profile on the Agulhas Bank, *Bull. Seismol. Soc. Am.*, *62*(4), 1029–1051.

Hales, A. L., and E. S. Sacks (1959), Evidence for an intermediate layer from crustal structure studies in the eastern Transvaal, *Geophys. J. Int.*, *2*, 15–33.

Hartnady, C. J. H., Z. Ben-Avraham, and J. Rogers (1992), Deep-ocean basins and submarine rises off the continental margin of south-eastern Africa: New geological research, *S. Afr. J. Sci.*, *88*, 534–539.

Hayes, D. F., P. L. Manley, J. W. Malin, and R. E. Houtz (1991), Crustal structure: Circum Antarctic to 30°S, in *Marine Geological and Geophysical Atlas of the Circum-Antarctic to 30°S*, edited by D. E. Hayes, pp. 21–24, AGU, Washington.

Hinz, K., S. Neben, Y. B. Gouseva, and G. A. Kudryavtsev (2004), A compilation of geophysical data from the Lazarev Sea and the Riiser-Larsen Sea, Antarctica, *Mar. Geophys. Res.*, *25*(3-4), 233–245, doi:10.1007/s11001-005-1319-y.

Hirsch, K. K., K. Bauer, and M. Scheck-Wenderoth (2009), Deep structure of the western South African passive margin—Results of a combined approach of seismic, gravity and isostatic investigations, *Tectonophysics*, *470*(1-2), 57–70, doi:10.1016/j.tecto.2008.04.028.

Hosseinpour, M., R. D. Muller, S. E. Williams, and J. M. Whittaker (2013), Full-fit reconstruction of the Labrador Sea and Baffin Bay, *Solid Earth*, *4*, 461–479.

Huebscher, C., W. Jokat, and H. Miller (1996), Crustal structure of the Antarctic continental margin in the eastern Weddell Sea, in *Weddel Sea Tectonics and Gondwana Breakup*, 108th ed., edited by B. C. Storey, E. C. King, and R. A. Livermore, pp. 165–174, Geol. Soc. London. Spec. Publ., London.

Hutchinson, D. R., J. A. Grow, K. D. Klitgord, and B. A. Swift (1983), *Deep Structure and Evolution of the Carolina Trough, in Studies in Continental Margin Geology*, vol. 34, edited by J. S. Watkins and C. L. Drake, pp. 129–152, AAPG Mem., Tulsa.

Ikami, A., K. Ito, and K. Kaninuma (1983), Deep crustal structure along the profile between Syowa and Mizuho stations, East Antarctica, *Mem. Natl. Inst. Polar Res.*, *28*(43), 19–28.

Ikami, A., K. Ito, K. Shibuya, and K. Kaninuma (1984), Crustal structure of the Mizuho Plateau, Antarctica, revealed by explosion seismic experiments, in *Antarctic Earth Science*, edited by R. L. Oliver, P. R. James, and J. B. Jago, pp. 509–513, Cambridge Univ. Press, Cambridge.

Jokat, W., T. Boebel, M. Konig, and U. Meyer (2003), Timing and geometry of early Gondwana breakup. *J. Geophys. Res.*, *108*(B9), 2428, doi:10.1029/2002JB001802.

Jokat, W., O. Ritzmann, C. Reichert, and K. Hinz (2004), Deep crustal structure of the continental margin off the Explora escarpment and in the Lazarev Sea, East Antarctica, *Mar. Geophys. Res.*, *25*(3-4), 283–304, doi:10.1007/s11001-005-1337-9.

Kamen-Kaye, M. (1983), Mozambique-Damagascar geosyncline, II: Petroleum geology, *J. Petroleum Geol.*, *5*(3), 287–308.

Kogan, A. L. (1972), Results of deep seismic sounding of the Earth's crust in east Antarctica, in *Antarctic Geology and Geophysics*, edited by R. J. Adie, pp. 485–489, Universitets Forlaget, Oslo.

König, M., and W. Jokat (2010), Advanced insights into magmatism and volcanism of the Mozambique Ridge and Mozambique Basin in the view of new potential field data, *Geophys. J. Int.*, *180*(1), 158–180, doi:10.1111/j.1365-246X.2009.04433.x.

Kristoffersen, Y., K. Strand, R. Vorren, D. Harwood, and P. Webb (2000), Pilot shallow drilling on the continental shelf, Dronning Maud Land, Antarctica, *Antarctic Sci.*, *4*, 463–470.

Kurinin, R. G., and G. E. Grikurov (1982), Crustal structure of part of East Antarctica from geophysical data, in *Symposium on Antarctic Geology and Geophysics-International Union of Geological Sciences*, 4th ed., edited by C. Craddock, pp. 895–901, Univ. Wisconsin Press, Madison.

Kydryavtzev, G. A., V. V. Butzenko, and I. N. Kadmina (1991), Crustal section across the Western Queen Maud Land continental margin from geophysical data, in *International Symposium on Antarctic Earth Sciences*, edited by Y. Yoshida, K. Kaminuma, and K. Shiraishi, pp. 330–335, Natl. Inst. Polar Res., Tokyo.

Leinweber, V. T., and W. Jokat (2011), Is there continental crust underneath the northern Natal Valley and the Mozambique Coastal Plains?, *Geophys. Res. Lett.*, *38*, L14303, doi:10.1029/2011GL047659.

Leinweber, V. T., and W. Jokat (2012), The Jurassic history of the Africa-Antarctica corridor—New constraints from magnetic data on the conjugate continental margins, *Tectonophysics*, *530–531*, 87–101, doi:10.1016/j.tecto.2011.11.008.

Leinweber, V. T., F. Klingelhoefer, S. Neben, C. Reichert, D. Aslanian, L. Matias, and W. Jokat (2013), The crustal structure of the Central Mozambique continental margin—Wide-angle seismic, gravity and magnetic study in the Mozambique channel, eastern Africa, *Tectonophysics*, *599*, 170–196, doi:10.1016/j.tecto.2013.04.015.

Leitchenkov, G., J. Guseva, V. Gandyukhin, G. Grikurov, Y. Kristoffersen, M. Sand, A. Golynsky, and N. Aleshkova (2008), Crustal structure and tectonic provinces of the Riiser-Larsen Sea area (East Antarctica): Results of geophysical studies, *Mar. Geophys. Res.*, *29*(2), 135–158, doi:10.1007/s11001-008-9051-z.

Li, X., R. Kind, and X. Yuan (2003), Seismic study of upper mantle and transition zone beneath hotspots, *Phys. Earth Planet. Interiors*, *136*(1–2), 79–92, doi:10.1016/S0031-9201(03)00021-9.

Ludwig, W. J., J. E. Nafe, E. S. W. Simpson, and S. Sacks (1968), Seismic refraction measurements on the southeast Africa continental margin, *J. Geophys. Res.*, *73*, 3707–3719, doi:10.1029/JB073i012p03707.

Mahanjane, E. S. (2012), A geotectonic history of the northern Mozambique Basin including the Beira High—A contribution for the understanding of its development, *Mar. Petrol. Geol.*, *36*(1), 1–12, doi:10.1016/j.marpetgeo.2012.05.007.

Marks, K. M., and A. A. Tikku (2001), Cretaceous reconstructions of East Antarctica, Africa and Madagascar, *Earth Planet. Sci. Lett.*, *186*, 479–495.

Marschall, H. R., C. J. Hawkesworth, C. D. Storey, B. Dhuime, P. T. Leat, H. P. Meyer, and S. Tamm-Buckle (2010), The Annandagstoppane granite, East Antarctica: Evidence for Archaean intracrustal recycling in the Kaapvaal-Grunehogna craton from zircon O and Hf isotopes, *J. Petrol.*, *51*(11), 2277–2301, doi:10.1093/petrology/egq057.

Martin, A. K., and C. J. H. Hartnady (1986), Cretaceous reconstructions of East Antarctica, Africa and Madagascar, *Earth Planet. Sci. Lett.*, *91*(B5), 479–495.

Maus, S., T. Sazonova, K. Hemant, J. D. Fairhead, and D. Ravat (2007), National geophysical data center candidate for the world digital magnetic anomaly map, *Geochem. Geophys. Geosyst.*, *8*, Q06017, doi:10.1029/2007GC001643.

McKenzie, D. (1978), Some remarks on the development of sedimentary basins, *Earth Planet. Sci. Lett.*, *40*, 25–32.

Miller, G. G., and V. Singh (1994), Potential field tilt-a new concept for location of potential field sources, *J. Appl. Geophys.*, *32*, 213–217.

Mjelde, R., T. Raum, B. Myhren, H. Shimamura, Y. Murai, T. Takanami, and U. Naess (2005), Continent-ocean transition on the Vøring Plateau, NE Atlantic, derived from densely sampled ocean bottom seismometer data, *J. Geophys. Res.*, *110*, B05101, doi:10.1029/2004JB003026.

Mooney, W. D., G. Laske, and T. G. Masters (1998), CRUST 5.1: A global crustal model at 5° × 5°, *J. Geophys. Res.*, *103*, 727–747, doi:10.1029/97JB02122.

Mougenot, D., M. Gennesseaux, J. Hernandez, C. Lepvrier, J. A. Malod, S. Raillard, J. R. Vanney, and M. Villeneuve (1991), La ride du Mozambique (Océan Indien): Un fragment continental individualisé lors du coulissement de l'Amérique et de l'Antarctique le long de l'Afrique de l'Est?, *C. R. Acad. Sci., Ser. II*, *312*, 655–662.

Mueller, C. O., B. Schreckenberger, I. Heyde, and W. Jokat (2015), The crustal structure of Beira High, Central Mozambique-combined investigation of wide-angle seismic and potential field data, AGU Gen. Assem., San Francisco, 14-18 Dec.

Müller, R. D., M. Sdrolias, C. Gaina, and W. R. Roest (2008), Age, spreading rates, and spreading asymmetry of the world's ocean crust, *Geochem. Geophys. Geosyst.*, *9*, Q04006, doi:10.1029/2007GC001743.

Nain, S. K., S. S. Gao, K. H. Liu, and P. G. Silver (2006), Southern African crustal evolution and composition: Constraints from receiver function studies, *J. Geophys. Res.*, *111*, B02304, doi:10.1029/2005JB003802.

Nguuri, T. K., D. E. James, S. J. Webb, C. Wright, T. G. Zengeni, O. Gwavava, and J. A. Snoke (2001), Crustal structure beneath southern Africa and its implications for the formation and evolution of the Kaapvaal and Zimbabwe cratons, *Geophys. Res. Lett.*, *28*, 2501–2504, doi:10.1029/2000GL012587.

Norton, I. O., and J. G. Sclater (1979), A model for the evolution of the Indian Ocean and the breakup of Gondwanaland, *J. Geophys. Res.*, *84*, 6803–6830, doi:10.1029/JB084iB12p06803.

Parker, R. L. (1973), The rapid calculation of potential anomalies, *Geophys. J. Int.*, doi:10.1111/j.1365-246X.1973.tb06513.x.

Parsiegla, N., J. Stankiewicz, K. Gohl, T. Ryberg, and G. Uenzelmann (2009), Southern African continental margin: Dynamic processes of a transform margin, *Geochem. Geophys. Geosyst.*, *10*, Q03007, doi:10.1029/2008GC002196.

Qui, X., K. Priestley, and D. McKenzie (1996), Average lithospheric structure of southern Africa, *Geophys. J. Int.*, *127*(3), 563–581.

Rabinowitz, P. D., and J. L. Labrecque (1977), Ocean-continent boundary at passive continental margins I, *Earth Planet. Sci. Lett.*, *35*, 145–150.

Rabinowitz, P. D., M. F. Coffin, and D. Falvey (1983), The separation of Madagascar and Africa, *Science*, *220*(4592), 67–69, doi:10.1126/science.220.4592.67.

Recq, M., J. Goslin, P. Charvis, and S. Operto (1998), Small-scale crustal variability within an intraplate structure, the Crozet Bank (southern Indian Ocean), *Geophys. J. Int.*, *134*, 145–156.

Reeves, C. V., and M. J. de Wit (2000), Making ends meet in Gondwana: Retracing the transforms of the Indian Ocean and reconnecting continental shear zones, *Terra Nova*, *12*(6), 272–282.

Roeser, A., J. Fritsch, and K. Hinz (1996), The development of the crust off Dronning Maud Land, East Antarctica, in *Weddell Sea Tectonics and Gondwana Break-Up*, vol. 108, edited by I. Stanisstreet, pp. 243–264, Geol. Soc. Spec. Publ., London.

Saki, T., Y. Tamura, S. Tokuhashi, T. Kodata, I. Mizukoshi, and H. Amano (1987), Preliminary report of geological and geophysical surveys off Queen Maud Land, East Antarctica, *Natl. Inst. Polar Res. Symp. Antarctica Geosci.*, 1, 23–40.

Sandwell, D. T., R. D. Müller, W. H. F. Smith, E. Garcia, and R. Francis (2014), New global marine gravity model from CryoSat-2 and Jason-1 reveals buried tectonic structure, *Science*, *346*(65), 65–67, doi:10.1126/science.1258213.

Schnabel, M., D. Franke, M. Engels, K. Hinz, S. Neben, V. Damm, and P. R. Dos Santos (2008), The structure of the lower crust at the Argentine continental margin, South Atlantic at 44°S, *Tectonophysics*, *454*(1–4), 14–22, doi:10.1016/j.tecto.2008.01.019.

Sclater, J. G., C. Jaupart, and D. Galson (1980), The heat flow through oceanic and continental crust and the heat loss of the Earth, *Rev. Geophys.*, *18*(1), 269–311, doi:10.1029/RG018i001p00269.

Segev, A. (2002), Flood basalts, continental breakup and the dispersal of Gondwana: Evidence for periodic migration of upwelling mantle flows (plumes), *EGU Stephan Mueller Spec. Publ. Ser.*, *2*, 171–191.

Segoufin, J. (1978), Anomalies magnetique mesozoique dans le bassin de Mozambique, *C.R. Sceances Acad. Sci., Ser. 2*, *287D*, 109–112.

Seton, M., R. D. Müller, S. Zahirovic, C. Gaina, T. Torsvik, G. Shephard, and M. Chandler (2012), Global continental and ocean basin reconstructions since 200 Ma, *Earth Sci. Rev.*, *113*(3–4), 212–270, doi:10.1016/j.earscirev.2012.03.002.

Simpson, E. S. W., J. G. Sclater, B. Parsons, I. Norton, and L. Meinke (1979), Mesozoic magnetic lineations in the Mozambique Basin, *Earth Planet. Sci. Lett.*, *43*(2), 260–264, doi:10.1016/0012-821X(79)90209-7.

Sinha, M. C., K. E. Louden, and B. Parsons (1981), The crustal structure of the Madagascar Ridge, *Geophys. J. Int.*, *66*(2), 351–377.

Smith, W. H. F., and D. T. Sandwell (1997), Global seafloor topography from satellite altimetry and ship depth soundings, *Science*, *277*, 1956–1962.

Steinhar, J. S., and R. P. Meyer (1961), *Explosion Studies of Continental Structure*, pp. 226–383, Carnegie Inst. Wash. Publ., Washington.

Stuart, G. W., and T. G. Zengeni (1987), Seismic crustal structure of the Limpopo mobile belt, Zimbabwe, *Tectonophysics*, *144*, 323–335.

Sutra, E., G. Manatschal, G. Mohn, and P. Unternehr (2013), Quantification and restoration of extensional deformation along the Western Iberia and Newfoundland rifted margins, *Geochem. Geophys. Geosyst.*, *14*, 2575–2597, doi:10.1002/ggge.20135.

Sykes, T. J. S. (1996), A correction for sediment lead upon the ocean floor: Uniform versus varying sediment density estimations—Implications for isostatic correction, *Mar. Geol.*, *133*(1–2), 35–49, doi:10.1016/0025-3227(96)00016-3.

Tedla, G. E., M. van der Meijde, A. A. Nyblade, and F. D. van der Meer (2011), A crustal thickness map of Africa derived from a global gravity field model using Euler deconvolution, *Geophys. J. Int.*, *187*, 1–9.

Tetreault, J. L., and S. J. H. Buiter (2014), Future accreted terranes: A compilation of island arcs, oceanic plateaus, submarine ridges, seamounts and continental fragments, *Solid Earth*, *5*, 1243–1275.

Trumbull, R. B., D. L. Reid, C. de Beer, D. van Acken, and R. L. Romer (2007), Magmatism and continental breakup at the west margin of southern Africa: A geochemical comparison of dolerite dikes from northwestern Namibia and the Western Cape, *South African J. Geol.*, *110*, 477–502.

Tucholke, B. E., R. E. Houtz, and D. M. Barrett (1981), Continental crust beneath the Agulhas Plateau, southwest Indian Ocean, *J. Geophys. Res.*, *86*, 3791–3806, doi:10.1029/JB086iB05p03791.

Veevers, J. J., J. W. Tayton, and B. D. Johnson (1985), Prominent magnetic anomaly along the continent-ocean boundary between the northwestern margin of Australia (Exmouth and Scott Plateaus) and the Argo Abyssal Plain, *Earth Planet. Sci. Lett.*, *72*(4), 415–426, doi:10.1016/0012-821X(85)90062-7.

Verduzco, B., J. D. Fairhead, C. M. Green, and C. M. MacKenzie (2004), New insights into magnetic derivatives for structural mapping, *Leading Edge*, *23*(2), 116–119, doi:10.1190/1.1651454.

Voss, M., and W. Jokat (2007), Continent-ocean transition and voluminous magmatic underplating derived from P-wave velocity modelling of the East Greenland continental margin, *Geophys. J. Int.*, *170*(2), 580–604, doi:10.1111/j.1365-246X.2007.03438.x.

Watts, A. B. (2001), Gravity anomalies, flexure and crustal structure at the Mozambique rifted margin, *Marine Petrol. Geol.*, *18*, 445–455.

Webb, S. J., R. G. Cawthorn, T. Nguuri, and D. James (2004), Gravity modeling of Bushveld complex connectivity supported by Southern African seismic experiment results, *South African J. Geol.*, *107*(1-2), 207–218, doi:10.2113/107.1-2.207.

Williams, S. E., J. M. Whittaker, and R. D. Müller (2011), Full-fit, palinspastic reconstruction of the conjugate Australian-Antarctic margins, *Tectonics*, *30*, TC6012, doi:10.1029/2011TC002912.

Zhao, M., C. A. Langston, A. A. Nyblade, and T. J. Owens (1999), Upper mantle velocity structure beneath southern Africa from modeling regional seismic data, *J. Geophys. Res.*, *104*, 4783–4794, doi:10.1029/1998JB900058.